

ผลของมวลโมเลกุลของโพลีออลต่อพฤติกรรมการกระเจิงแสงแบบผันกลับได้เชิงความร้อนของเบนซอก
ซาซีน-ยูรีเทนโคพอลิเมอร์



นายกิตติภณ บุญญานุวัฒน์

จุฬาลงกรณ์มหาวิทยาลัย

บทคัดย่อและแฟ้มข้อมูลฉบับเต็มของวิทยานิพนธ์ตั้งแต่ปีการศึกษา 2554 ที่ให้บริการในคลังปัญญาจุฬาฯ (CUIR)
เป็นแฟ้มข้อมูลของนิสิตเจ้าของวิทยานิพนธ์ ที่ส่งผ่านทางบัณฑิตวิทยาลัย

The abstract and full text of theses from the academic year 2011 in Chulalongkorn University Intellectual Repository (CUIR)
are the thesis authors' files submitted through the University Graduate School.

วิทยานิพนธ์นี้เป็นส่วนหนึ่งของการศึกษาตามหลักสูตรปริญญาวิศวกรรมศาสตรมหาบัณฑิต

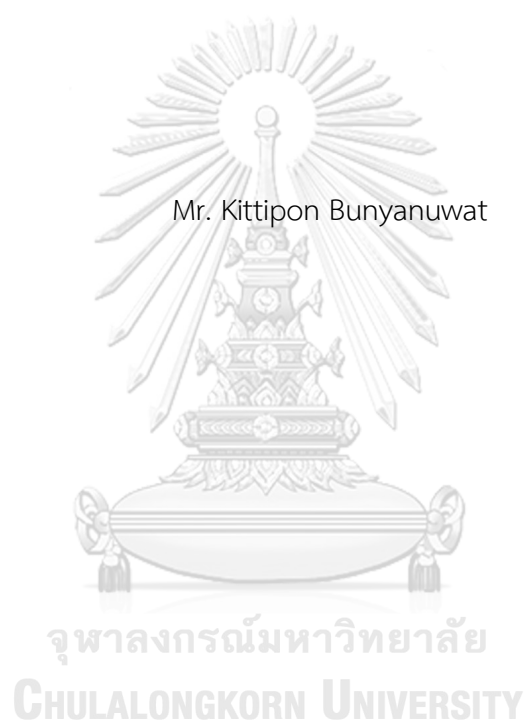
สาขาวิชาวิศวกรรมเคมี ภาควิชาวิศวกรรมเคมี

คณะวิศวกรรมศาสตร์ จุฬาลงกรณ์มหาวิทยาลัย

ปีการศึกษา 2560

ลิขสิทธิ์ของจุฬาลงกรณ์มหาวิทยาลัย

Effects of polyol molecular weights on thermally reversible light scattering behaviors
of benzoxazine-urethane copolymers



A Thesis Submitted in Partial Fulfillment of the Requirements
for the Degree of Master of Engineering Program in Chemical Engineering

Department of Chemical Engineering

Faculty of Engineering

Chulalongkorn University

Academic Year 2017

Copyright of Chulalongkorn University

กิตติภณ บุญญานุวัฒน์ : ผลของมวลโมเลกุลของโพลีออลต่อพฤติกรรมการกระเจิงแสงแบบผันกลับได้เชิงความร้อนของเบนซอกซาซีน-ยูรีเทนโคพอลิเมอร์ (Effects of polyol molecular weights on thermally reversible light scattering behaviors of benzoxazine-urethane copolymers) อ.ที่ปริกษานิพนธ์หลัก: ศ. ดร. ศรารุช ริมดุสิต, 82 หน้า.

พฤติกรรมการกระเจิงของแสงแบบผันกลับได้ด้วยความร้อนของเบนซอกซาซีน-ยูรีเทนโคพอลิเมอร์ถูกศึกษาในงานวิจัยนี้ เบนซอกซาซีนมอนอเมอร์ถูกสังเคราะห์ด้วยเทคนิคการสังเคราะห์แบบปราศจากตัวทำละลายโดยใช้สารตั้งต้นเป็นบิสฟีนอลเอ, พาราฟอร์มัลดีไฮด์, และ อนิซีน ซึ่งมีอัตราส่วนโดยโมลอยู่ที่ 1:4:2 ตามลำดับ ยูรีเทนพรีพอลิเมอร์ถูกเตรียมได้จากการทำปฏิกิริยาระหว่างพอลิพรพิลีนไกลคอล ซึ่งมีมวลโมเลกุลอยู่ที่ 1000, 2000, และ 3000 กรัมต่อโมล กับโทลูอีนไดไอโซไซยาเนตโดยใช้อัตราส่วนโมลอยู่ที่ 1:2 ตามลำดับ ภายใต้บรรยากาศไนโตรเจน โดยกำหนดสัญลักษณ์แทนที่มวลโมเลกุล 1000, 2000 และ 3000 เป็น PU1K และ PU2K และ PU3K ตามลำดับ เบนซอกซาซีนมอนอเมอร์และยูรีเทนพรีพอลิเมอร์สามารถเชื่อมต่อกันด้วยพันธะเคมีเกิดเป็นโครงร่างตาข่ายสามมิติได้ระหว่างการให้ความร้อนในการบ่ม หมู่ฟังก์ชันที่เชื่อมต่อกันระหว่างเบนซอกซาซีนมอนอเมอร์และยูรีเทนพรีพอลิเมอร์ถูกศึกษาโดยเทคนิคเอทีอาร์ เอฟทีไออาร์สเปกโทรสโกปี และ รามานไมโครสเปกโทรสโกปี ปฏิกิริยาการเชื่อมต่อเป็นโครงข่ายของเบนซอกซาซีนกับยูรีเทนจะแสดงกราฟเป็นพิคคายความร้อนเมื่อทำการตรวจวัดด้วยเทคนิคดีเฟอเรนเชียลสแกนนิ่งแคลอริเมทรี อุณหภูมิในการบ่มของเบนซอกซาซีนกับยูรีเทนนั้นมีค่าเพิ่มขึ้นเมื่อสัดส่วนโดยโมลของยูรีเทนในโคพอลิเมอร์เพิ่มขึ้น สารผสมระหว่างเบนซอกซาซีนกับยูรีเทนถูกบ่มอย่างสมบูรณ์เมื่อใช้การบ่มแบบทีละขั้นตั้งแต่อุณหภูมิ 160 องศาเซลเซียส จนถึง 200 องศาเซลเซียส ใช้เวลา 2 ชั่วโมงในแต่ละอุณหภูมิ อัลลอยด์ของเบนซอกซาซีนและยูรีเทนแสดงเสถียรภาพทางความร้อนที่สูงขึ้นเมื่อศึกษาจากเครื่องวิเคราะห์การเปลี่ยนแปลงน้ำหนักของสารโดยอาศัยคุณสมบัติทางความร้อน อัลลอยด์ของเบนซอกซาซีนและยูรีเทนที่มีมวลโมเลกุลสามพันกรัมต่อโมล ที่สัดส่วนโดยมวลของยูรีเทนพรีพอลิเมอร์เท่ากับ 30%, 40%, และ 50% สามารถเกิดปรากฏการณ์การกระเจิงของแสงแบบผันกลับได้ด้วยความร้อน อัลลอยด์ของเบนซอกซาซีนและยูรีเทนที่มีมวลโมเลกุลสามพันกรัมต่อโมล ที่สัดส่วนโดยมวลของยูรีเทนพรีพอลิเมอร์เท่ากับ 30% ณ อุณหภูมิห้องจะอยู่ในสถานะที่ก่อให้เกิดการกระเจิงแสง แต่เมื่อให้ความร้อนจนอุณหภูมิของชิ้นงานมีค่าเท่ากับ 128 องศาเซลเซียส อัลลอยด์ของเบนซอกซาซีนและยูรีเทนจะเปลี่ยนเป็นสถานะโปร่งใส เมื่ออัลลอยด์ถูกทำให้เย็นลง ณ ที่อุณหภูมิห้อง อัลลอยด์นั้นจะกลับมาทึบแสงอีกครั้ง อัลลอยด์ของเบนซอกซาซีนและยูรีเทนเกิดการแยกวัฏภาคซึ่งสามารถตรวจสอบได้จากเครื่องวิเคราะห์สมบัติของวัสดุเชิงกลทางความร้อน อัลลอยด์ของเบนซอกซาซีนและยูรีเทนมีพื้นฐานเป็นแบบอนุภาคพอลิเมอร์ระดับไมโครเมตร และ อยู่ในรูปร่างแบบพอลิเมอร์เดนไดรท์ซึ่งทำให้เกิดการกระเจิงของแสง โครงสร้างเหล่านี้สามารถตรวจสอบได้กล้องจุลทรรศน์แบบใช้แสงในโหมดส่องผ่านและโหมดส่องผ่านแบบใช้แสงโพลาไรซ์ ดังนั้นอัลลอยด์ของเบนซอกซาซีนและยูรีเทน ที่ถูกพัฒนาในงานวิจัยนี้สามารถนำไปใช้เป็นวัสดุตรวจจับความร้อนที่อุณหภูมิสูงได้

ภาควิชา วิศวกรรมเคมี

ลายมือชื่อนิสิต

สาขาวิชา วิศวกรรมเคมี

ลายมือชื่อ อ.ที่ปรึกษาหลัก

ปีการศึกษา 2560

5671032721 : MAJOR CHEMICAL ENGINEERING

KEYWORDS: BENZOXAZINE, URETHANE, THERMALLY REVERSIBLE LIGHT SCATTERING

KITTIPON BUNYANUWAT: Effects of polyol molecular weights on thermally reversible light scattering behaviors of benzoxazine-urethane copolymers. ADVISOR: PROF. SARAWUT RIMDUSIT, Ph.D., 82 pp.

The thermally reversible light scattering behaviors of benzoxazine-urethane copolymer was investigated in this work. Benzoxazine monomers (BA-a) were synthesized by the solventless synthesis technique from bisphenol-A, para-formaldehyde, and aniline with the molar ratio of 1:4:2, respectively. Urethane prepolymer was prepared by reacting poly(propylene glycol) ($M_w = 1000, 2000, \text{ or } 3000 \text{ g/mol}$) with toluene diisocyanate (TDI) at the molar ratio of 1:2 under a nitrogen atmosphere. The obtained urethane prepolymer (PU) was labelled as PU1K, PU2K, and PU3K with respect to the molecular weights of polyether polyol employed in the preparation step. Urethane prepolymer and benzoxazine monomers were crosslinked during the thermal curing by the urethane linkages as confirmed by ATR FT-IR spectroscopy and Raman microspectroscopy. The network forming reaction of the BA-a/PU binary mixture occurred simultaneously as a single exothermic peak was observed in the differential scanning calorimetry (DSC) thermograms. The curing temperature of BA-a/PU binary mixtures increased when PU mass fraction increased. The BA-a/PU binary mixtures were completely cured when a step-by-step thermal curing protocols were employed. The BA-a/PU alloys exhibited improved thermal stability due to the presence of BA-a as observed by the thermogravimetric analysis. Furthermore, polybenzoxazine-urethane alloys with PU3K mass fractions of 30%, 40%, and 50% exhibited thermally reversible light scattering phenomena. It was observed that BA-a/PU3K alloy at 30% wt of urethane shifted from the opaque state at room temperature to the transparent state when the temperature of the specimen was raised to 128°C. Transparent PU3K/BA-a alloys became opaque when the specimens were left to cool down to room temperature. BA-a/PU3K alloys were phase-separated from some fractions of PU3K as observed from the dynamic mechanical analysis. BA-a/PU3K alloys in the form of micrometer polymeric particles and dendritic morphology were the light scatters in our system as exhibited in the optical micrographs in transmission and cross-polarized transmission modes. Consequently, BA-a/PU3K alloys developed from this research are a promising candidate for applying in a high thermal sensing application.

Department: Chemical Engineering

Student's Signature

Field of Study: Chemical Engineering

Advisor's Signature

Academic Year: 2017

ACKNOWLEDGEMENTS

I wish to express my deep appreciation to my advisor, Prof. Dr. Sarawut Rimdusit for his kindness, invaluable supervision, guidance, advice, and encouragement throughout the course of this study and editing of this thesis.

My sincere gratitude is to Assoc. Prof. Dr. Varong Pavarajarn, Dr. Palang Bumroongsakulsawat and Asst. Prof. Dr. Chanchira Jubsilp for their instructive advices as my thesis committee.

This research is financially supported by Ratchadaphiseksomphot Endowment Fund of Chulalongkorn University and the polyol and isocyanate were kindly supplied by IRPC Co., Ltd.

Additionally, I would like to acknowledge my colleagues especially Dr. Tewarak Parnklang, Miss Phattarin Mora, Mr. Noppawat Kuengputpong, Mr Jakkrit Jantaramaha, and Mr. Peerawat Prathumrat for assistance and useful comments on my thesis. Everyone in Polymer Engineering Laboratory, Department of Chemical Engineering, Faculty of Engineering, Chulalongkorn University is highly appreciated for his invaluable discussion and friendly encouragement.

Finally, I would like to affectionately give my gratitude to my family for their wholehearted understanding, patience, and encouragement throughout my entire study.

CONTENTS

	Page
THAI ABSTRACT	iv
ENGLISH ABSTRACT	v
ACKNOWLEDGEMENTS	vi
CONTENTS	vii
CHAPTER I	1
Introduction	1
1.1 Light Scattering History	1
1.2 Thermally Reversible Light Scattering	2
1.3 Benzoxazine –Urethane Alloys for TRLS	3
1.4 Objectives	5
1.5 Scope of Research	5
1.6 Procedures of the study	6
CHAPTER II	8
Theory	8
2.1 The Mechanics of Light Scattering	8
2.2 Beer–Lambert law	9
2.3 Thermotropic Materials base on Light Scattering	10
2.4 Benzoxazine Resin	11
2.5 Polyurethane	15
2.6 Polyurethane Prepolymer Technique	16
2.7 Raw material	19
2.7.1 Isocyanate	19

	Page
2.7.2 Polyol.....	21
2.7.3 Bisphenol A.....	22
2.7.4 Formaldehyde.....	23
2.7.5 Aniline	23
2.8 Crosslinking between Benzoxazine Resin and Urethane Prepolymer	25
CHAPTER III	27
Literature Reviews	27
CHAPTER IV.....	38
EXPERIMENTAL	38
4.1 Raw Materials.....	38
4.2 Specimen Preparation.....	39
4.2.1 Benzoxazine Resin Preparation	39
4.2.2 Urethane Prepolymer Preparation	39
4.2.3 Benzoxazine:Urethane Prepolymer Binary Mixture Preparation.....	40
4.3 Characterizations.....	40
4.3.1 Attenuated Total Reflection Fourier Transform Infrared Spectroscopy (ATR FT-IR).....	40
4.3.2 Raman Spectroscopy	41
4.3.3 Optical Images and Optical Microscopy.....	41
4.3.4 Differential Scanning Calorimetry (DSC)	42
4.3.5 Light Scattering Apparatus.....	42
4.3.6 Dynamic Mechanical Analysis (DMA).....	43
4.3.7 Thermogravimetric Analysis (TGA)	43

	Page
CHAPTER V	44
RESULTS AND DICUSSION	44
5.1 Differential scanning calorimetry for curing condition observation	44
5.2 Optical Images	47
5.3 Optical Microscopy	48
5.4 Light scattering apparatus	50
5.5 ATR FT-IR and Raman Spectra	51
5.6 Dynamics Mechanical Analysis (DMA).....	54
5.7 Thermal Degradation and Thermal Stability Investigation	56
CHAPTER VI.....	58
CONCLUSIONS	58
REFERENCES	76
VITA.....	82

LIST OF FIGURE

Figure	Page
Figure 1.1 Thermo-optical property of TRLS film: (a) off-state and (b) on-state.....	2
Figure 1.2 Thermally reversible light scattering applications:	3
Figure 2.1 The Phenomenon of Light Scattering.....	9
Figure 2.2 Thermotropic switching by phase separation or phase transition in permanent domains.	10
Figure 2.3 Synthesis of monofunctional benzoxazine monomer.....	11
Figure 2.4 Synthesis of bifunctional benzoxazine monomer.	12
Figure 2.5 Ring-opening polymerization of monofunctional benzoxazine monomer.....	13
Figure 2.6 Ring-opening polymerization of bifunctional benzoxazine monomer.....	14
Figure 2.7 Urethane linkage.....	16
Figure 2.8 Polyurethane addition reaction.	16
Figure 2.9 Polyurethane prepolymer preparation.	16
Figure 2.10 Formation of high molecular weight polyurethane by the reaction of urethane prepolymer with oligo-diol.	17
Figure 2.11 Formation of high molecular weight polyurethane by the reaction of urethane prepolymer with water.	17
Figure 2.12 Polymerization of PU prepolymer by a reaction with water.	18
Figure 2.13 2,4- and 2,6-toluene diisocyanate (TDI).....	19
Figure 2.14 Structure of Polypropylene glycol.....	22
Figure 2.15 Synthesis of bisphenol A.....	22

Figure 2.16 Synthesis of aniline by nitrobenzene.....	24
Figure 2.17 Synthesis of aniline by phenol.....	24
Figure 2.18 Reaction of Cm-type polybenzoxazine and PU prepolymer.....	26
Figure 3.1 %T obtained in one thermo-cycle of the TRLS film.....	27
Figure 3.2 Opaque (a) and transparent (b) TRLS films.....	28
Figure 3.3 Plot of %T at 660 nm versus the number of cooling-heating cycles for a 1-mm thick TRLS film with dispersed 10 wt.% of 1-octadecanol.....	28
Figure 3.4 Optical transmittance at a wavelength of 660 nm as a function of the contents of 1-octadecanol crystallites.....	29
Figure 3.5 Tensile strength as a function of the contents of OD crystallites.....	30
Figure 3.6 Transmission optical micrographs of TRLS films synthesized using 55 wt.% and NP 3 wt.% PS obtained at room temperature (a) and 85°C (b).....	30
Figure 3.7 Intensity of transmitted light as a function of temperature in successive heating/cooling cycles at 5 °C/min for a 200 µm-thickness TRLS film containing 55 wt.% NP and 3 wt.% PS.....	31
Figure 3.8 Intensity of transmitted light as a function of time in successive heating/cooling cycles at 5 °C/min for a 200 µm-thickness TRLS film containing 55 wt.% NP and 3 wt.% PS.....	32
Figure 3.9 Intensity of transmitted light as a function of temperature during heating and cooling cycles at 2 °C/min for a 270 µm-thickness TRLS film containing 50 wt.% EBBA and 1 wt.% PS.....	33
Figure 3.10 DCS thermograms of BA-a/PU with the weight ratio 100/0 (a), 90/10 (b), 80/20 (c), 70/30 (d), 60/40 (e).....	33
Figure 3.11 Temperature dependence of optical transmission spectra and optical micrographs along with schematic views from 200°C to room temperature.....	34
Figure 3.12 Optical transmittance as a function of temperature for a 200-µm thick film containing 30 wt.% C20 by heating/cooling cycle at 20°C/min.....	35

Figure 3.13 %Transmittance as a function of time during successive heating/cooling cycles at 20 °C/min for a 200- μ m thick TRLS film containing 30 wt.% C20.....	36
Figure 3.14 Relationship between M_n of polyol and glass transition temperature of BA:PU alloys from differential scanning calorimeter: (\blacklozenge) $M_n = 1000$, (\blacksquare) $M_n = 2000$, (\blacktriangle) $M_n = 3000$, and (\bullet) $M_n = 5000$ g/mol.....	37
Figure 3.15 TGA thermograms of the BA:PU (80:20) polymer alloys at various number average molecular weights of polyol: (\blacktriangledown) Pure BA, (\blacklozenge) $M_n = 1000$, (\blacksquare) $M_n = 2000$,.....	37
Figure 5.1 DSC thermograms of benzoxazine-urethane resin mixtures at various BA-a:PU3K mass ratios: (\bullet)100:0, (\blacksquare)90:10, (\blacklozenge)80:20, (\blacktriangle)70:30, (\blacktriangledown)60:40, (\blacktriangleleft)50:50, and (\blacktriangleright)40:60.....	60
Figure 5.2 DSC thermograms of benzoxazine-urethane resin mixtures at 40:60 mass ratio at various curing conditions: (\blacktriangledown)Uncured, (\bullet)130°C 1hr, (\blacksquare)150°C 1hr, (\blacklozenge)160°C 2hr, (\blacktriangle)170°C 2hr, (\blacktriangleright)180°C 2hr, and (\blacktriangleleft)200°C 2hr.	61
Figure 5.3 Thermally reversible light scattering behaviors of BA-a/PU2K.....	62
Figure 5.4 Optical micrographs of 100- μ m thick PU3K (A–C), polybenzoxazine (D–F), 60%PU3K/BA-a (G–I), and 30%PU3K/BA-a films in reflection, transmission, and cross-polarized transmission modes. The magnifications of all micrographs are 20X. The scale bars in all micrographs are 200 μ m.	63
Figure 5.5 Optical micrographs of 100- μ m thick 30%PU3K/BA-a films in reflection (A and D), transmission (B and E), and cross-polarized transmission (C and F) modes. The magnifications of the micrographs are 20X (A–C) and 50X (D–F). The scale bars in A–C and D–F are 200 μ m and 500 μ m, respectively.....	64
Figure 5.6 Thermo-optical curve of BA-a/PU2K alloys at 30wt%: (\bullet) Heating and (\blacksquare) Cooling	65
Figure 5.7 Thermo-optical curve of BA-a/PU2K alloys at 40wt%: (\bullet) Heating and (\blacksquare) Cooling	66

Figure 5.8 Thermo-optical curve of BA-a/PU3K alloys at 30wt%: (●) Heating and (■) Cooling	67
Figure 5.9 Thermo-optical curve of BA-a/PU3K alloys at 40wt%: (●) Heating and (■) Cooling	68
Figure 5.10 Thermo-optical curve of BA-a/PU3K alloys at 50wt%: (●) Heating and (■) Cooling	69
Figure 5.11 ATR FT-IR spectra (A) and Raman spectra (B) of BA-a resin, polybenzoxazine, PU3K prepolymer, and BA-a/PU3K alloys at various PU3K mass fractions.	71
Figure 5.12 Storage modulus of BA-a:PU3K copolymers at various mass ratios: (●)100:0, (■)70:30, (◆)60:40, (▲)50:50 and (▼)0:100.....	72
Figure 5.13 Loss modulus of BA-a:PU3K copolymers at various mass ratios: (●)100:0, (■)70:30, (◆)60:40, (▲)50:50 and (▼)0:100.....	73
Figure 5.14 Loss tangent of BA-a:PU3K copolymers at various mass ratios: (●)100:0, (■)70:30, (◆)60:40, (▲)50:50 and (▼)0:100.....	74
Figure 5.15 TGA thermograms of BA-a/PU3K alloys at various compositions: (●)100:0, (■)70:30, (◆)60:40 and (▲)50:50.....	75

LIST OF TABLE

Table	Page
Table 2.1 The specification of toluene diisocyanate.....	20
Table 5.1 Visual appearance of BA-a/PU alloys at room temperature.	62
Table 5.2 Transition temperature of BA-a/PU2K and BA-a/PU3K at various alloy mass ratios.	70



CHAPTER I

Introduction

1.1 Light Scattering History

Principle of light scattering was initiated by Lord Rayleigh (1842–1919), who was both theoretician and an experimentalist to correctly explain the color of the sky. In order for light to be scattered in a given system, there must be some permute in the refractive index at the point from which light is scattered. Scattering also takes place in a continuously homogeneous medium of small particles or molecules because the particles are continuously undergoing Brownian motion and randomly moving. Rayleigh's work was subsequently elaborated by Debye (1915) and Gans (1925). Later, Einstein and Smoluchowski learned that on a mesoscopic scale, macroscopic properties such as density, pressure, concentration, and even temperature undergo fluctuations which, in turn, affected the refractive index and cause light to scatter [1].

1.2 Thermally Reversible Light Scattering

Thermally reversible light scattering materials (TRLS) are intelligent materials that can be switched from opaque state (off-state) to transparent state (on-state) by varying temperature (Figure 1.1).

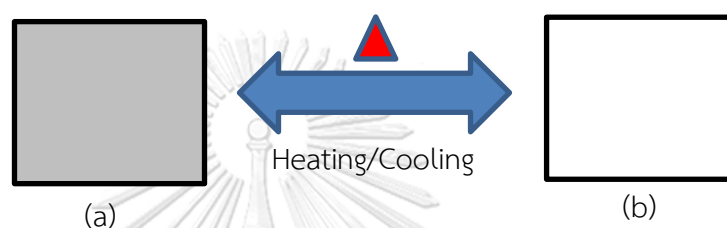


Figure 1.1 Thermo-optical property of TRLS film: (a) off-state and (b) on-state.

From this characteristic, TRLS have potential applications in thermal sensors, optical devices, recording media, and several other applications [[2],[3],[4],[5],[6]] (Figure 1.2). TRLS film generally consists of a support polymer matrix with dispersed domains of relatively low molar mass species e.g. liquid crystal [[7],[8],[9],[10]] polymer blend [11], hydrogel [[12]-[13]], and phase change materials (PCMs), which might be fatty acid, inorganic eutectics, and paraffin [[14], [15], [16]]. Changing between transparent (on-state) and scattering states (off-state) is accomplished by a change in refractive index of one or both components, a change in the aggregate state, or by reversible solid-liquid phase formation of PCMs at different temperatures.



Figure 1.2 Thermally reversible light scattering applications:

(a) Shutter and (b) Thermal sensor

1.3 Benzoxazine –Urethane Alloys for TRLS

Polybenzoxazine is a novel kind of thermosetting phenolic resin. The new type of phenolic resin has distinctive characteristics such as molecular design flexibility, low moisture absorption, near zero-volume shrinkage upon polymerization, low melt viscosities, no by-product during curing, and ability to alloy with various types of resin. In addition, it can be synthesized using the solventless technology to yield a clean precursor without the need of monomer purification. Consequently, it can be applied in various fields of stringent property requirements such as electronic, automotive, or construction industries. However, polybenzoxazine still has some intrinsic shortcomings, including its brittleness as a consequence of the short molecular weight of the network structure. Alloying of elastomeric materials to this brittle resin has been reported to effectively improve its flexibility. Urethane

elastomer, flexible epoxy, or anhydride compounds are examples of flexibility enhancer of the polymer [17].

Urethane elastomer, which is a family of segmented polymers with hard segment derived from isocyanates and soft segment derived from polyols, exhibits excellent flexibility and high abrasion resistance. However, urethane elastomer has low moisture resistance and poor thermal stability [[18],[19],[20]]. Urethane prepolymer can form a network by reacting with moisture in the atmosphere. The polymer alloy of benzoxazine resin (BA) and urethane prepolymer (PU) is a very attractive polymer hybrid system because synergism in glass transition temperature (T_g) was observed at about 30 wt.% of the urethane prepolymer. The presence of PU renders greater cross-linked density in the polymer alloys. In addition, the BA-a/PU system also exhibits enhanced thermal stability relating to the thermal sensor application. The aim of this research is to investigate the TRLS behavior in benzoxazine resin alloyed with urethane resin i.e. BA-a/PU system. This system is very appealing for some optical applications besides its prominent mechanical and thermal characteristics.

1.4 Objectives

1. To study effects of diol molecular weights on thermal and optical properties of polymer alloys between benzoxazine resin and urethane resin for thermally reversible light scattering (TRLS) applications.
2. To evaluate effects of urethane resin contents on thermal and optical properties of the TRLS polymer alloys based on benzoxazine and urethane resins.

1.5 Scope of Research

1. Synthesis of BA-a typed benzoxazine resin by the solventless synthesis technique.
2. Synthesis of urethane prepolymer using three different molecular weight of diols ($M_w = 1000, 2000, 3000$) and toluene diisocyanate (TDI).
3. Investigation of thermally reversible light scattering property of benzoxazine-urethane alloys with various weight ratios of urethane and benzoxazine resins i.e. PU:BA-a of 0:100, 10:90, 20:80, 30:70, 40:60, 50:50, and 60:40.
4. Evaluation of the effects of polyol molecular weights on curing and crosslink behaviors of urethane-benzoxazine alloys.
 - Determining functional groups (ATR FT-IR and Raman spectroscopy)
5. Investigation of thermal, mechanical and optical properties of the obtained TRLS specimens.

5.1 Thermal properties

- Curing behaviors and glass transition temperature (Differential scanning calorimeter and Dynamic mechanical analyzer)

- Thermal degradation temperature and thermal stability (Thermogravimetric analyzer)

5.2 Mechanical properties

- Dynamic mechanical properties (Dynamic mechanical analyzer)

5.3 Optical properties

- Optical Image (Digital camera)

- Optical micrographs (Microscope)

- Thermo-optical curve (Light scattering apparatus)

1.6 Procedures of the study

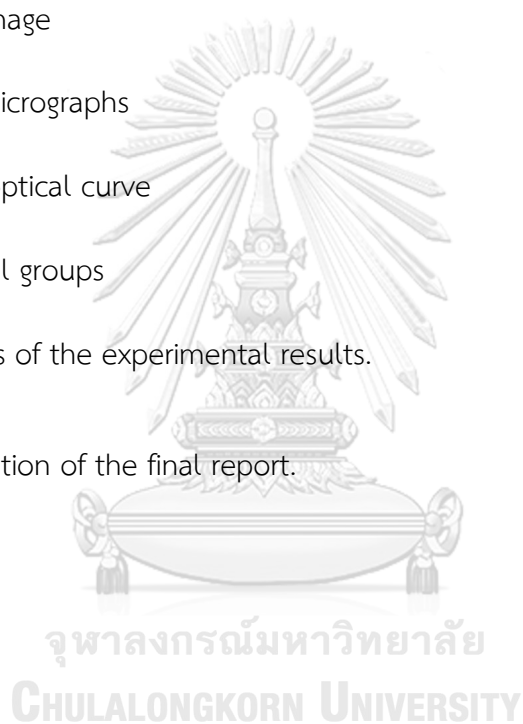
1. Reviewing related literature.
2. Preparation of chemicals and equipment for using in this research.
3. Synthesis of benzoxazine resins (BA-a) and urethane prepolymers.
4. Preparation of poly(benzoxazine-urethane).

5. Determination of thermal, mechanical and optical properties of poly(benzoxazine-urethane) as follows:

- Glass transition temperature
- Thermal degradation temperature
- Dynamic mechanical properties
- Optical Image
- Optical micrographs
- Thermo-optical curve
- Functional groups

6. Analysis of the experimental results.

7. Preparation of the final report.



CHAPTER II

Theory

2.1 The Mechanics of Light Scattering

The light scattering is the alteration of the direction and intensity of a light beam that strikes an object. The alteration is due to the combined effects of reflection, refraction, and diffraction used as shown in Figures 2.1 [21]. This reduction in the energy of the incident beam leads to the concept of extinction, which is the degree of attenuation of the incident light energy.

Total energy of incident beam

$$E_{\text{incident}} = E_{\text{transmitted}} + E_{\text{extinction}}$$

E_{incident} is the total energy of incident beam

$E_{\text{transmitted}}$ is the transmitted energy of incident beam

$E_{\text{extinction}}$ is the loss energy of incident beam

Loss energy of incident beam

$$\text{Extinction} = \text{scattering} + \text{absorption}$$

where scattering = reflection + refraction + diffraction

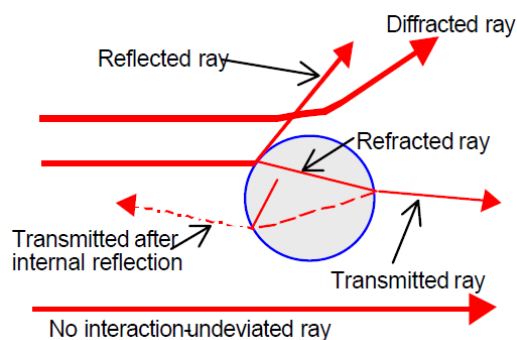


Figure 2.1 The Phenomenon of Light Scattering

Both scattering and absorption cause the incident light beam to be diminished as it is projected through an assemblage of particles, some decrease due to redirection of rays by scattering, some decrease due to the loss of the photons by absorption.

2.2 Beer–Lambert law

By definition, the transmittance (T) of material sample is

$$T = \frac{I_{\text{transmitted}}}{I_{\text{incident}}}$$

$I_{\text{transmitted}}$ is the radiant flux transmitted by that material sample.

I_{incident} is the radiant flux impinged upon that material sample.

2.3 Thermotropic Materials base on Light Scattering

Thermotropic materials switch between a highly transparent state and a light scattering state. In the light scattering state, domains exhibiting a refractive index different from the refractive index of the matrix material are present. These domains can appear by a phase separation process. In addition, the domains can be permanent and change their refractive index at the thermotropic switching temperature. In the latter case the refractive indexes of matrix and domain are equal in the transparent state and differ in the light scattering state [22].

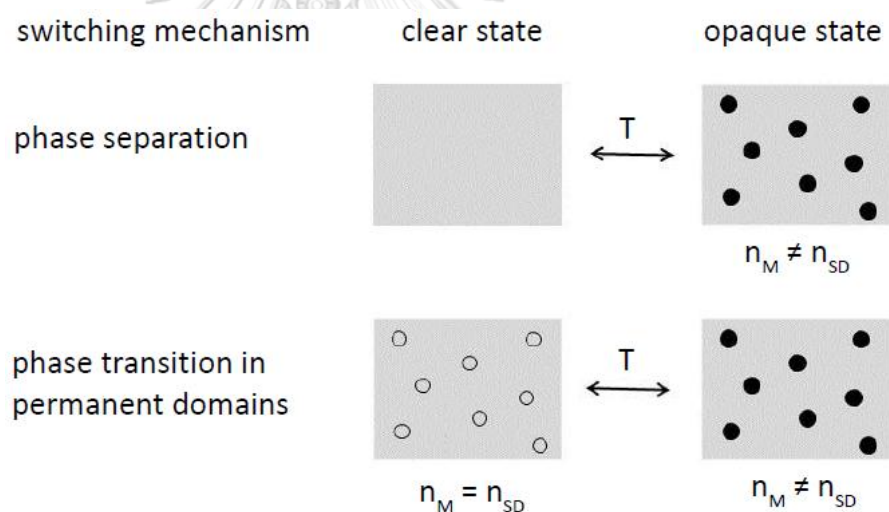


Figure 2.2 Thermotropic switching by phase separation or phase transition in permanent domains.

2.4 Benzoxazine Resin

Benzoxazine resin is a novel kind of phenolic resin that can be synthesized from phenol, formaldehyde, and amines [23]. Solvent may be used in this synthesis depending on initiator and heating [24]. The resin is developed to provide optimal properties in electronics and high thermal stability applications.

Benzoxazine resin can be classified into a monofunctional and a bifunctional type depending on a type of phenol used as shown in Figures 2.3 and 2.4.

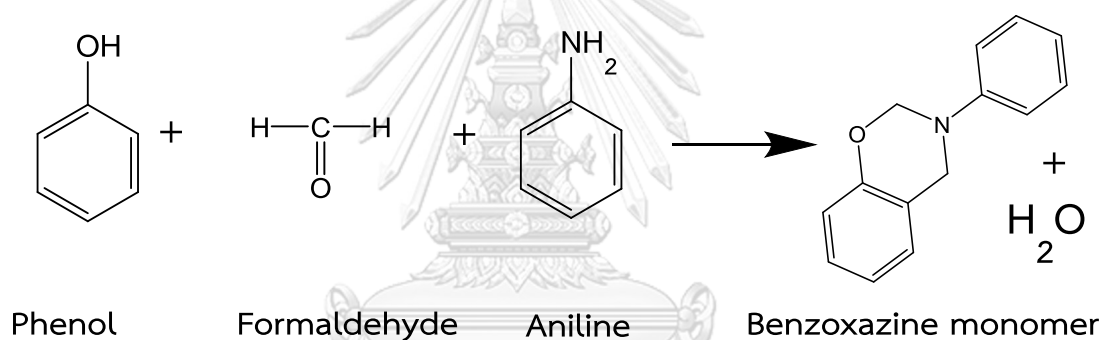


Figure 2.3 Synthesis of monofunctional benzoxazine monomer.

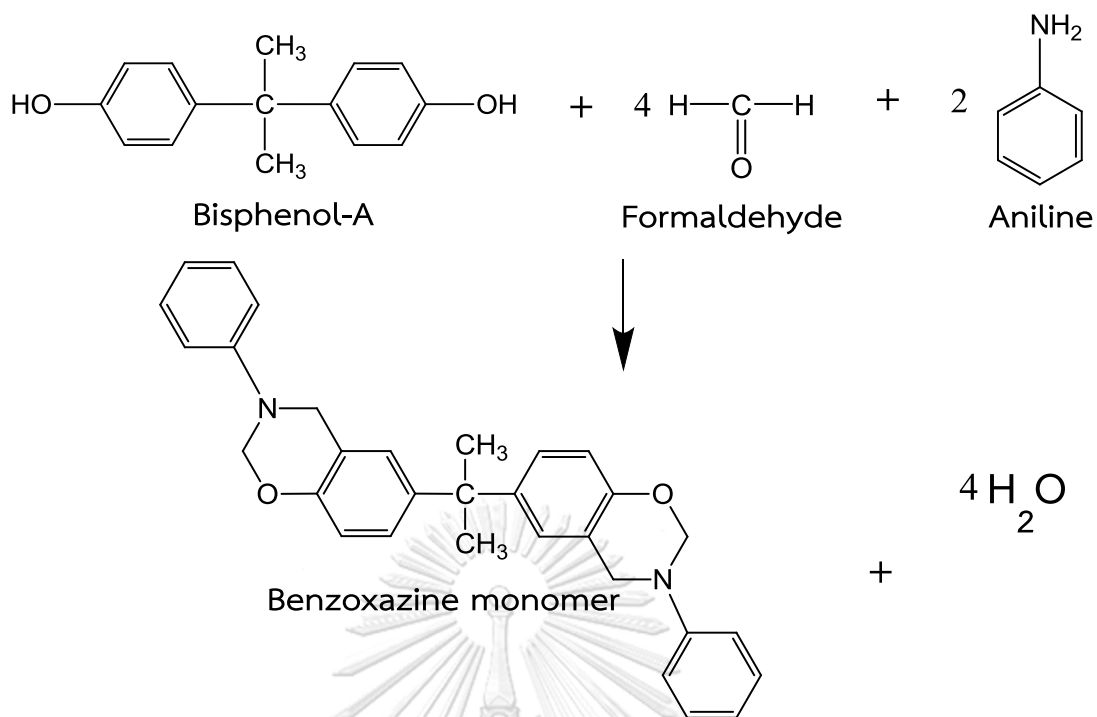


Figure 2.4 Synthesis of bifunctional benzoxazine monomer.

The benzoxazine resin allows development of new applications due to their unique superior properties such as [23]

- Solventless synthesis provides almost contaminant-free monomer.
- Self-polymerized upon heating.
- No catalyst or curing agent required.
- No by-products during cure.
- Low melt viscosity.
- Near zero-volume shrinkage.
- Low water absorption.
- Excellent electrical properties.

- High mechanical integrity.

The benzoxazine monofunctional monomers can be polymerized to yield a linear structure (Figure 2.5). The benzoxazine bifunctional monomer can be subsequently polymerized to yield a network structure (Figure 2.6). Benzoxazine resin was reported to be able to alloy with several other polymer or resin. Consequently, the polymer alloys including polybenzoxazine with bisphenol A-typed epoxy [25], flexible epoxy (EPO732) [20], isophorone diisocyanate (IPDI)/polyether polyol-typed urethane resin [20], toluene diisocyanates (TDI)/polyethylene adipate polyol-typed urethane resin [19], with polyimide [26], rendered a broader range of useful properties.

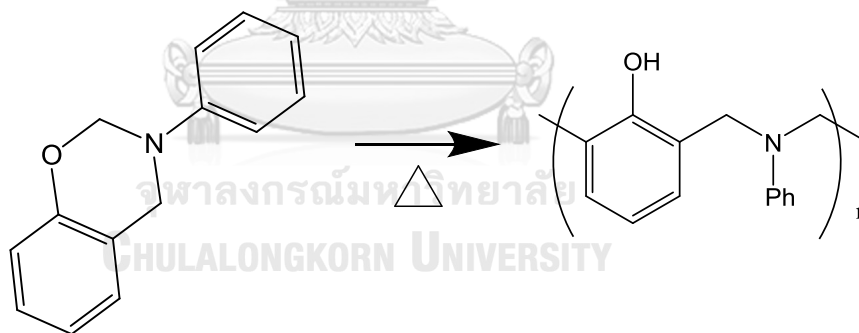


Figure 2.5 Ring-opening polymerization of monofunctional benzoxazine monomer.

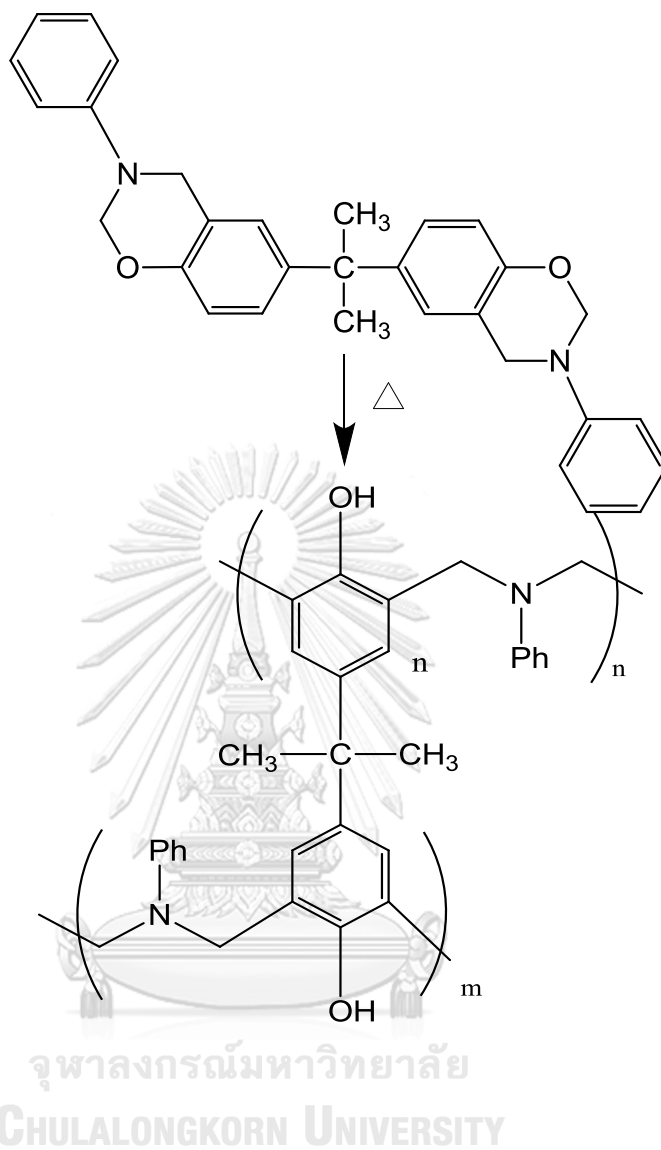


Figure 2.6 Ring-opening polymerization of bifunctional benzoxazine monomer.

2.5 Polyurethane

Polyurethane is a polymer that contains urethane functional group (-NH-CO-O-). Polyurethane consisting of soft and hard segments are formed by the addition polymerization between diols or polyols (i.e. soft segment) and diisocyanate or polyisocyanate (i.e. hard segment) (Figure 2.8) [27]. The rate of the polymerization reaction depends upon the structure of both the isocyanate and the polyol. The functionality of the hydroxyl-containing reactants or the isocyanate can be varied. As a result, a wide variety of linear branched and crosslinked structures can be formed. The hydroxyl-containing components cover a wide range of molecular weight and types, including polyester and polyether polyols. Aliphatic polyols with primary hydroxyl end-groups are the most reactive. They react with isocyanate faster than similar polyols with secondary hydroxyl groups. The polyfunctional isocyanate can be aromatic, aliphatic, cycloaliphatic, or polycyclic in structure and can react with any compound containing "active" hydrogen atoms. This flexibility in the selection of reactants of polyurethane also leads to its wide range of properties of polyurethane. Polyurethane have excellent flexibility, outstanding resistance, high abrasion resistance. Nevertheless, polyurethane exhibits low resistance to moisture and poor thermal stability. Polyurethane is employed in many applications such as automotive, furniture, construction, thermal insulation and footwear [28].

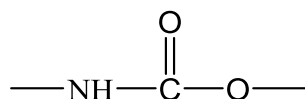


Figure 2.7 Urethane linkage

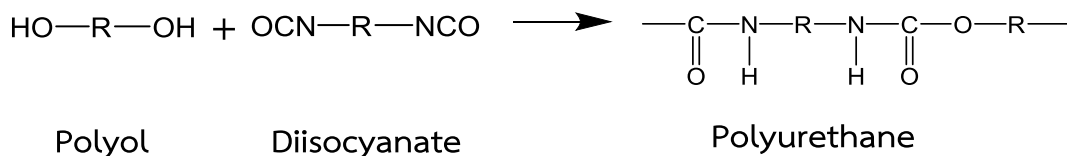


Figure 2.8 Polyurethane addition reaction.

2.6 Polyurethane Prepolymer Technique

Prepolymers of polyurethane are formed by the reaction of a diisocyanate with an oligo-polyol, at the molar [diisocyanate]/[OH group] of 1/1 [29]. In fact, only one group of diisocyanate reacts with one hydroxyl group of the polyol. A structure with free terminal-NCO groups called 'prepolymer' is produced.

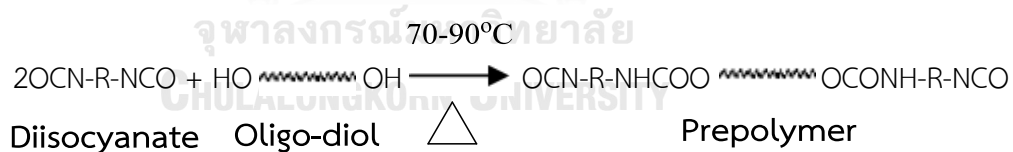


Figure 2.9 Polyurethane prepolymer preparation.

High molecular weight polyurethanes are formed by the reaction of a prepolymer with a chain extender e.g. ethylene glycol, diethylene glycol, 1,4-butanediol, or diamine,.

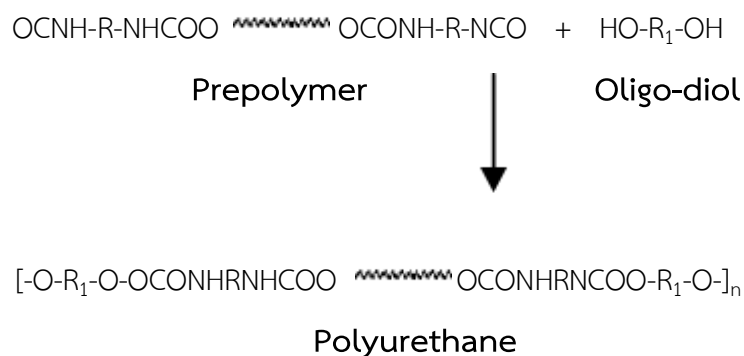


Figure 2.10 Formation of high molecular weight polyurethane by the reaction of urethane prepolymer with oligo-diol.

The prepolymer can also be extended to a high molecular weight polymer by reaction with water present in the atmosphere. In fact, water is a chain extender and the resulting high molecular weight polymer has both bonds: urethane and urea bonds. If a prepolymer derived from an oligo-triol or an oligo-polyol, having three or more terminal NCO groups is used, crosslinked polyurethanes will be obtained when the prepolymer is exposed to the atmospheric humidity (Figure 2.11 and 2.12)

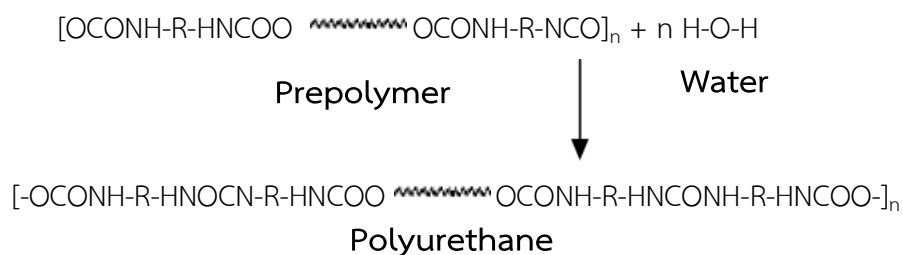


Figure 2.11 Formation of high molecular weight polyurethane by the reaction of urethane prepolymer with water.

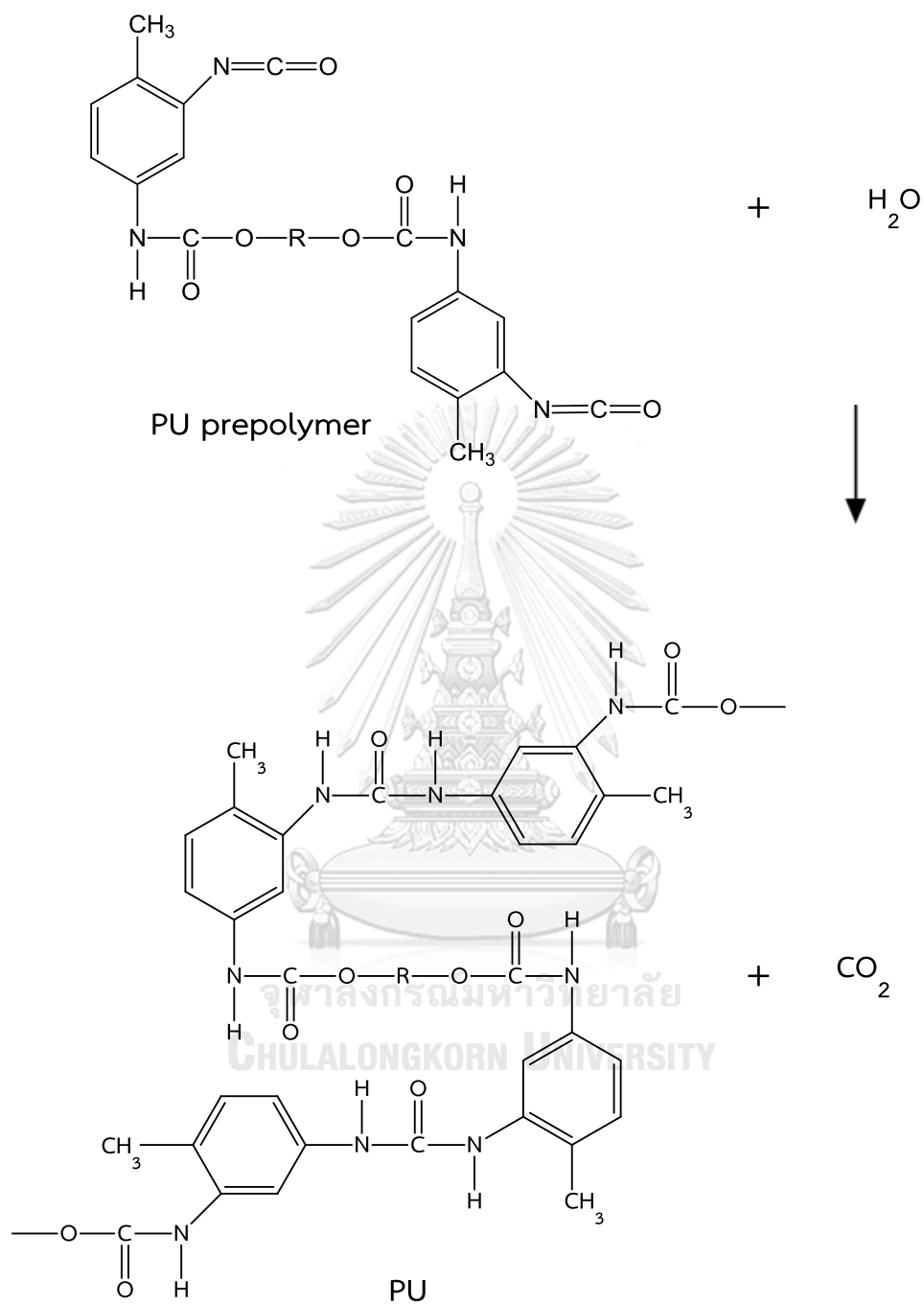


Figure 2.12 Polymerization of PU prepolymer by a reaction with water.

2.7 Raw material

In this work, raw materials employed for the synthesis of PU prepolymer are toluene diisocyanate (TDI) and polyether diol with molecular weights of 1000, 2000, and 3000 g/mol

2.7.1 Isocyanate

Toluene Diisocyanate (TDI)

TDI is an aromatic diisocyanate. Most of the TDI used is a mixture of 2,4- and 2,6-diisocyanates. The structure formula of toluene diisocyanate (TDI) are shown in Figure 2.13 [30].

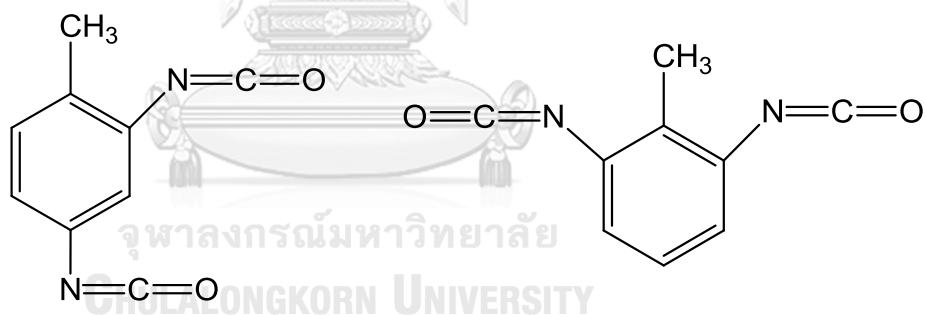


Figure 2.13 2,4- and 2,6-toluene diisocyanate (TDI)

Toluene diisocyanate is prepared by direct nitration of toluene to give a 80:20 mixture of the 2,4- and 2,6-dinitro derivatives, followed by hydrogenation to the corresponding diaminotoluene. Though toluene diisocyanate (TDI) is stable with a relatively high-flash point, it can be reacted with water, acid, base, organic, and

inorganic compounds. The 80:20 mixture of 2,4-TDI and 2,6-TDI is the most important commercial product. The specifications of toluene diisocyanate are shown in Table 2.1 [29] [31].

Table 2.1 The specification of toluene diisocyanate.

Properties	Value
Molecular weight	174.16
NCO content (% by weight)	48.3
Purity (% by weight)	99.5
Melting point ($^{\circ}\text{C}$)	19-22
Boiling point ($^{\circ}\text{C}$)	251
Density (g/cm^3)	1.22 at 20°C
Viscosity ($\text{mPa}\cdot\text{s}$)	3.2 at 20°C
Vapor pressure (Pa)	3.3 at 25°C

2.7.2 Polyol

The polyols employed to make polyurethanes have been developed to have the required reactivity with commercially available isocyanate and to produce polyurethanes with specific properties. A wide range of polyols is used in polyurethane manufacturing. Most of the polyols used fall into two classes: hydroxyl-terminated polyethers, or hydroxyl-terminated polyesters. The structure, molecular weights, and functionality of the polyol play are crucial in determining the properties of the final urethane polymer.

Polyether Polyols

Polyether polyols containing the repeating ether linkage (-R-O-R-) have two or more hydroxyl groups as terminal functional groups. They are manufactured commercially by the catalyzed addition of epoxies (cyclic ethers) to an initiator. The most important types of the cyclic ethers are propylene oxide and ethylene oxide. Butylene oxide is also employed. These oxides react with active hydrogen-containing compounds (called initiators), such as water, glycols, polyols and amines. Thus, a wide variety of compositions of varying structures, chain lengths and molecular weight is theoretically possible. By selecting the proper oxide (or oxides), initiators, reaction conditions, and catalysts, it is possible to synthesize a series of polyether polyols ranging from low-molecular-weight polyglycols to high-molecular-weight resins. Most polyether polyols are produced for polyurethane application. In this

work, the polyol used for the synthesis of our urethane prepolymer is polypropylene glycol (MW = 1000, 2000, and 3000 g/mol). The structural formula of the polypropylene glycol are shown in Figure 2.14.

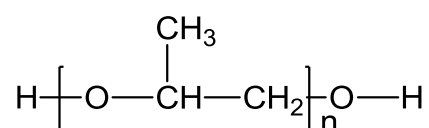


Figure 2.14 Structure of Polypropylene glycol

2..7.3 Bisphenol A

Bisphenol A is produced by reacting phenol with acetone in the presence of an acid catalyst (shown in Figure 2.15). Common catalysts are aqueous acids or acid clays. Promoters such as thioglycolic acid and resorcinol are also used [32].

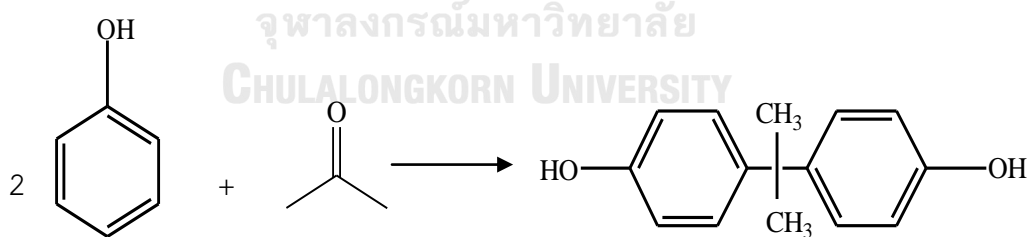
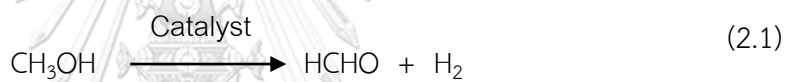


Figure 2.15 Synthesis of bisphenol A.

2.7.4 Formaldehyde

Formaldehyde is an unstable colorless gas, which is commercially supplied in 37% aqueous solution, as a solid cyclic trimer (trioxan), and as a solid polymer (paraformaldehyde) which used in this work. Almost all formaldehyde produced is derived from methanol either by oxidative dehydrogenation using silver or copper catalyst (see Equation 2.1), or by oxidation in the presence of Fe_2O_3 and MoO_3 (see Equation 2.2) [32].



In the oxidative dehydrogenation, the generated hydrogen is oxidized to water upon addition of air.



2.7.5 Aniline

The classical method of synthesis of aniline is the reduction of nitrobenzene with hydrogen in the vapor phase using a copper/silica catalyst (shown in Figure 2.16).

Nitrobenzene is produced in the nitration of benzene using a mixture of nitric acid and sulfuric acid [32].

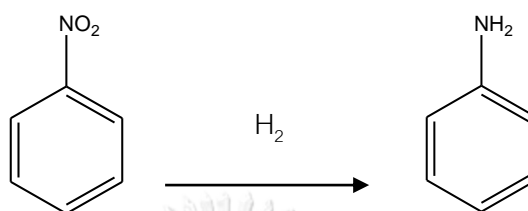


Figure 2.16 Synthesis of aniline by nitrobenzene.

Recently Aristech Chemical completed a 90,000-ton aniline plant using plant using phenol as the feedstock. This technology was developed by Halcon; it is also used by Mitsui Toatsu in Japan. The amination of phenol is conducted in the vapor phase using an alumina catalyst, and yield are very high.

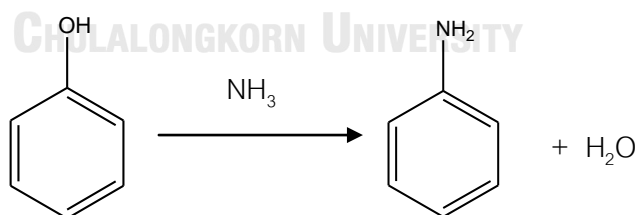


Figure 2.17 Synthesis of aniline by phenol.

2.8 Crosslinking between Benzoxazine Resin and Urethane Prepolymer

Previously, Takeichi and co-workers [19] studied the synthesis and characterization of poly(urethane-benzoxazine) film. The poly(urethane-benzoxazine) film as novel polyurethane (PU)/phenolic resin alloys were prepared by blending a benzoxazine monomer (BA-a) and TDI-polyethylene adipate polyol (MW = 1000) based PU prepolymer. The mechanism of benzoxazine-urethane alloys was proposed by model reaction of monofunctional benzoxazine monomer, 3,4-dihydro-3,6-dimethyl-2H-1,3-benzoxazine (CM) and phenyl isocyanate. FT-IR spectroscopic technique was used to investigate the reaction between benzoxazine resin and urethane prepolymer. The main structures in benzoxazine-urethane alloys were considered to be a crosslinking between NCO of the PU prepolymer and phenolic hydroxyl groups from ring-opening polymerization of BA-a. The mechanism of benzoxazine-urethane alloys was proposed as illustrated in Figure 2.18 [19].

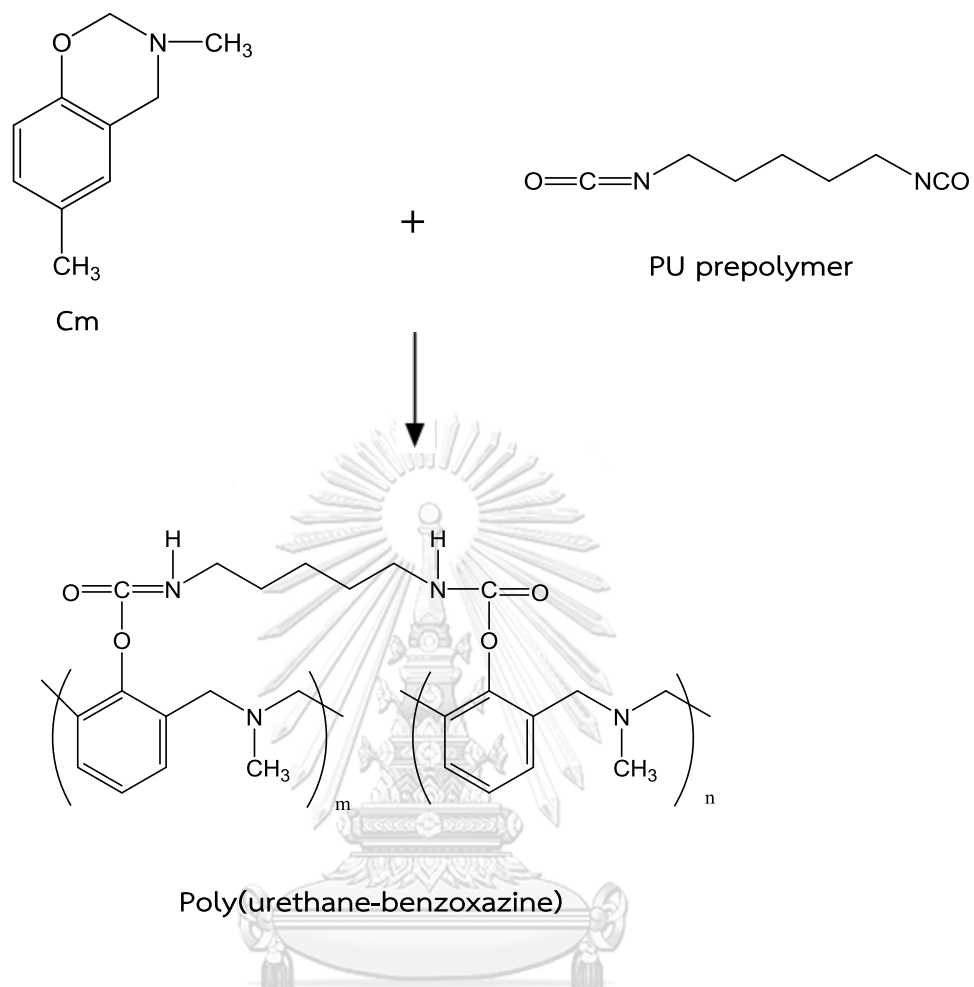


Figure 2.18 Reaction of Cm-type polybenzoxazine and PU prepolymer.

CHAPTER III

Literature Reviews

L. Cao, M. Mou, G.Feng and Y.Wang [33] studied UV-cured polyether urethane diacrylate (PEUDA) with dispersed 1-octadecanol (OD) as a thermally reversible light scattering (TRLS) film. The TRLS film was opaque when temperature was below 45°C. With the increase of temperature at 5°C min⁻¹, the film became gradually transparent, and the transmittance at wavelength 660 nm (T_{660}) increased to over 90.0% when the temperature was above 60°C (Figure 3.1).

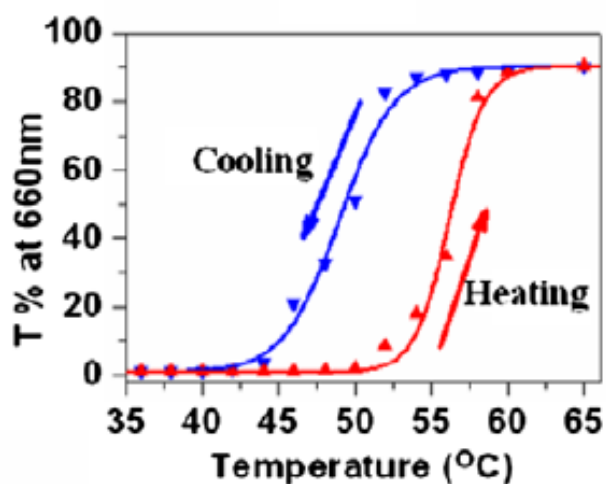


Figure 3.1 %T obtained in one thermo-cycle of the TRLS film.

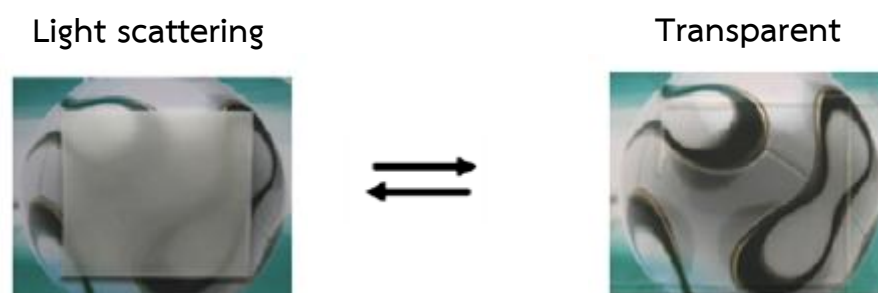


Figure 3.2 Opaque (a) and transparent (b) TRLS films.

The thermo-optical performance of a 1-mm thick TRLS film containing 10 wt% of 1-octadecanol in response to successive cyclic switching between opaque and transparent states was shown in Figure 3.3. Optical transmittance of the film at the two optically different states remained stable, about 1 T% and 92 T%, respectively, after 100 repeated heating/cooling cycles.

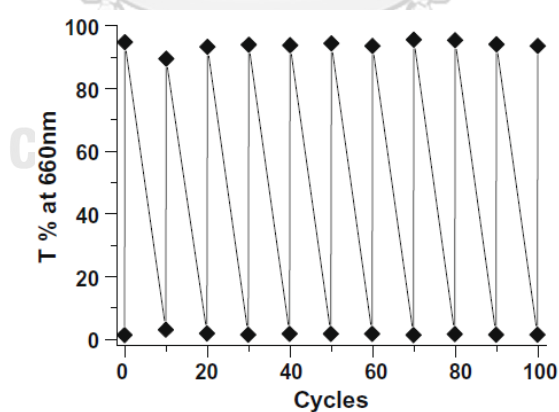


Figure 3.3 Plot of %T at 660 nm versus the number of cooling-heating cycles for a 1-mm thick TRLS film with dispersed 10 wt.% of 1-octadecanol.

The transparency of the TRLS film can be improved by varying the initial weight ratio of OD/PEUDA (Figure 3.4). The transmittance of the TRLS films at 25°C (opaque states) sharply decreased from 91%T to 2 %T when OD content increased from 0 to 10 wt.%. When OD content further increased over 20 wt.%, the transmittance was level-off. The transmittance of these films at 60°C (transparent states) with the value of 91 %T was almost invariable with the content of OD. Therefore, the transmittance in the two optical states increase with the increasing of OD/PEUDA ratio. The tensile strength of the 1-mm thick TRLS film steadily decreased with increment of OD/PEUA ratio and reached to 1.8 MPa when the content of OD exceeded 30 wt.% (Figure 3.5).

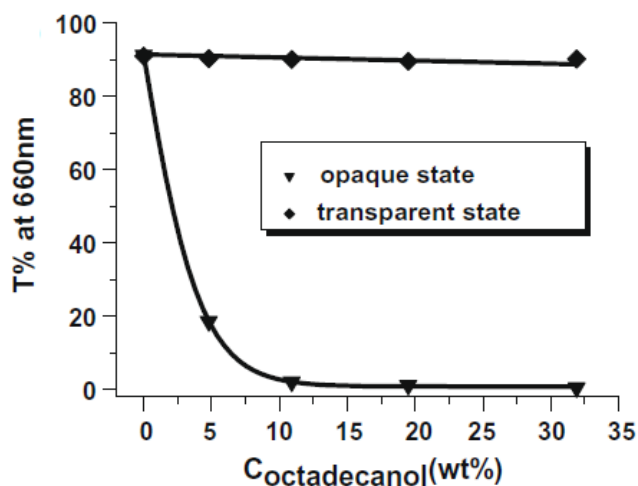


Figure 3.4 Optical transmittance at a wavelength of 660 nm as a function of the contents of 1-octadecanol crystallites.

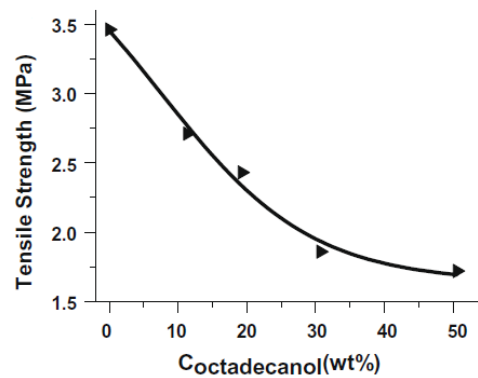


Figure 3.5 Tensile strength as a function of the contents of OD crystallites.

I.A. Zucchi, T. Resnik, P.A. Oyanguren, M.J. Galante, R.J.J. Williams [34] compared the optical properties of polystyrene (PS)/naphthalene (NP) domains or polystyrene/liquid crystal (EBBA) domains in epoxy matrices. Morphologies generated in the films synthesized using naphthalene (NP) are shown in Figure 3.6. Dispersed domains are constituted by an NP/PS solution that is rich in naphthalene. At room temperature, NP was crystallized inside dispersed domains. Therefore, dispersed domains scattered light and appeared opaque. Heating above the NP melting point (81°C) rendered the film transparent as the refractive index of NP was similar to the refractive index of epoxy.

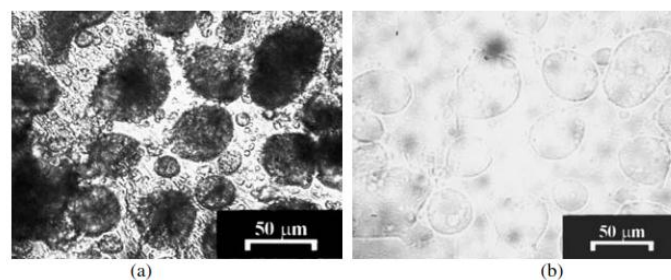


Figure 3.6 Transmission optical micrographs of TRLS films synthesized using 55 wt.% and NP 3 wt.% PS obtained at room temperature (a) and 85°C (b).

Figure 3.7 shows the variation of the intensity of the transmitted light as a function of temperature for a 200 μm -thick TRLS film containing 55 wt.% NP and 3 wt.% PS. Successive heating/cooling cycles were performed at $5^\circ\text{C}/\text{min}$. During a heating cycle, NP crystallization took place in the $50\text{--}70^\circ\text{C}$ temperature range, increasing the fraction of crystals in dispersed domains. Therefore, the transmittance of the TRLS film decreased. Melting of NP crystals began at about 70°C and was completed at 81°C , producing a transparent TRLS film. In the subsequent cooling cycle, NP crystallization took place at about 48°C leading to a very sharp decrease in the intensity of transmitted light. This behavior was quite reproducible for the selected rate of temperature change, as is shown in Figure 3.8 where variations in intensity during different heating/cooling cycles are plotted as a function of time.

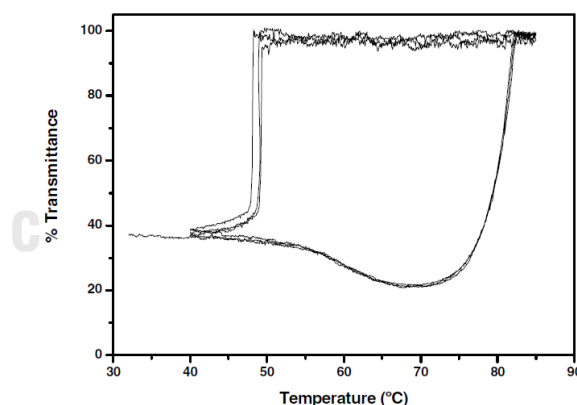


Figure 3.7 Intensity of transmitted light as a function of temperature in successive heating/cooling cycles at $5^\circ\text{C}/\text{min}$ for a 200 μm -thickness TRLS film containing 55 wt.% NP and 3 wt.% PS.

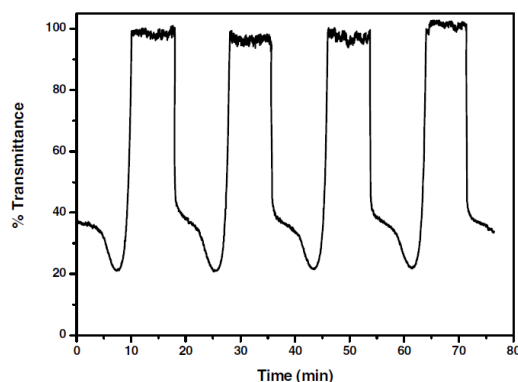


Figure 3.8 Intensity of transmitted light as a function of time in successive heating/cooling cycles at 5 °C/min for a 200 μm -thickness TRLS film containing 55 wt.% NP and 3 wt.% PS.

Figure 3.8 shows the intensity of transmitted light as a function of temperature during heating and cooling cycles at 2°C/min for a 270 μm -thick TRLS film containing 50 wt. % EBBA and 1 wt.% PS [33]. The thermal gap between transparent and opaque states is extremely reduced with respect to the case of using an organic crystal. A low undercooling (2–3°C) is enough to produce nematic domains inside dispersed particles. Evidently, the change in orientation of EBBA molecules that leads to a bidimensional array occurs much more rapidly than the organization of tridimensional organic crystals.

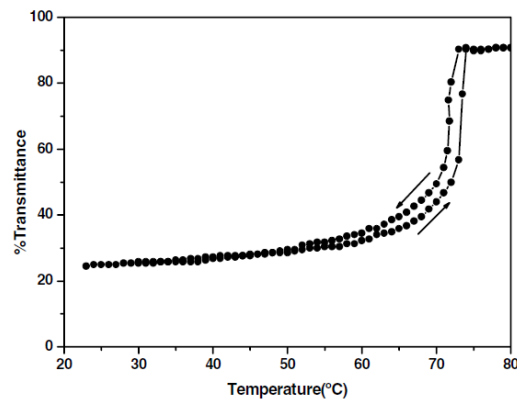


Figure 3.9 Intensity of transmitted light as a function of temperature during heating and cooling cycles at 2 °C/min for a 270 μm -thickness TRLS film containing 50 wt.% EBBA and 1 wt.% PS.

P.Kasemsiri, J.Wakita, S.Ando, and S. Rimdusit [35] investigated the thermally reversible light scattering characteristics of benzoxazine-urethane alloys (BA-a/PU). The glass transition temperature (T_g) of BA-a/PU increased when the PU content increased. In particular, the highest T_g of 240°C was obtained from 40 wt.% of PU (Figure 3.10).

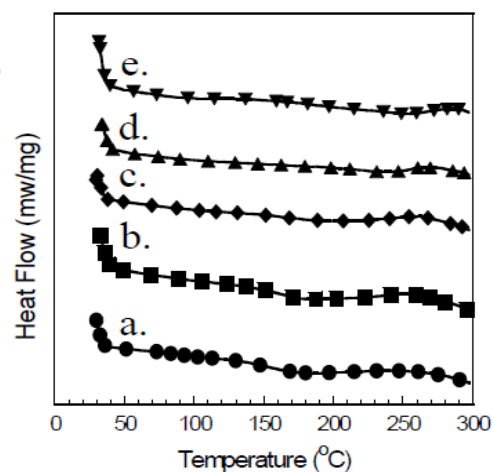


Figure 3.10 DCS thermograms of BA-a/PU with the weight ratio 100/0 (a), 90/10 (b), 80/20 (c), 70/30 (d), 60/40 (e).

At 200°C, the film became transparent without microphase separation. Furthermore, the transmittance at 500–700 nm was significantly higher than the value at room temperature. When film was cooled down to 150°C, the micro-phase separation re-appeared, and gradually became opaque at 100°C, 50°C, and room temperature. Therefore, the micro-phases separation at lower temperatures and transition to homogenous phase at evaluated temperature lead to TRLS behaviors to BA-a/PU system.

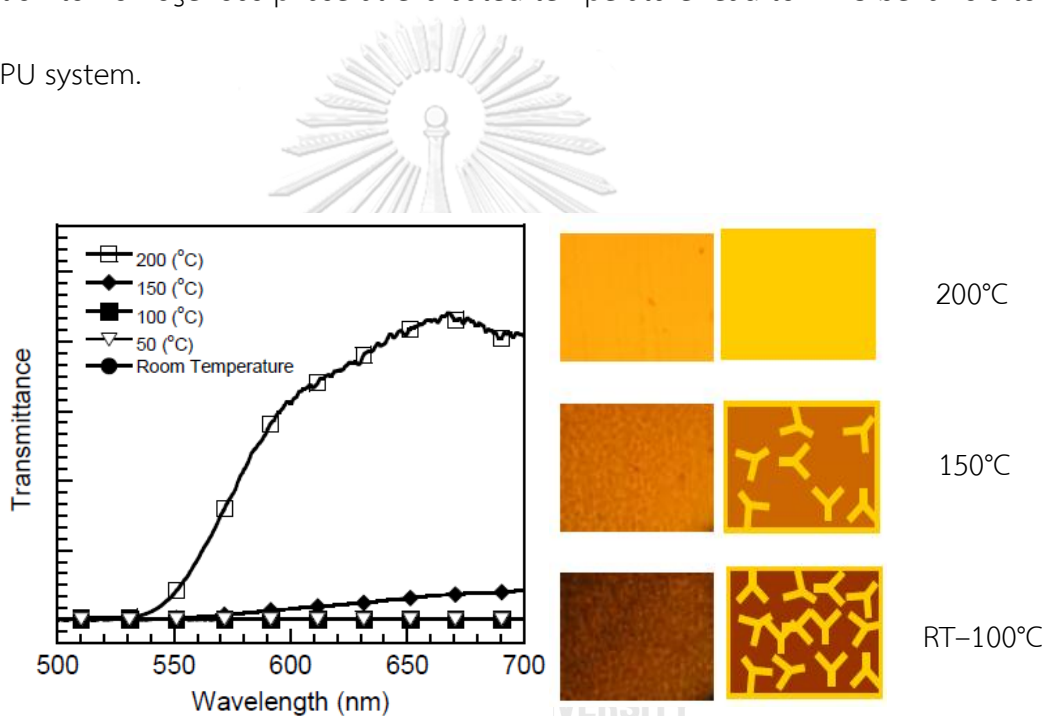


Figure 3.11 Temperature dependence of optical transmission spectra and optical micrographs along with schematic views from 200°C to room temperature.

J. Puig and coworkers [36] studied poly(dodecyl methacrylate) as a solvent of paraffin for phase change materials and thermally reversible light scattering films. The 200- μm thick TRLS film containing 30 wt.% C20 was subjected to a heating and cooling cycle at 20°C/min. The film became opaque in the range of 23–27°C during the cooling stage and transparent in the range of 30–35°C during the heating step. The opaque–transparent switching behavior occurred with a high reproducibility for successive heating–cooling cycles (Figure 3.13). This was due to the absence of leakage or agglomeration of the paraffin during the consecutive thermal cycles.

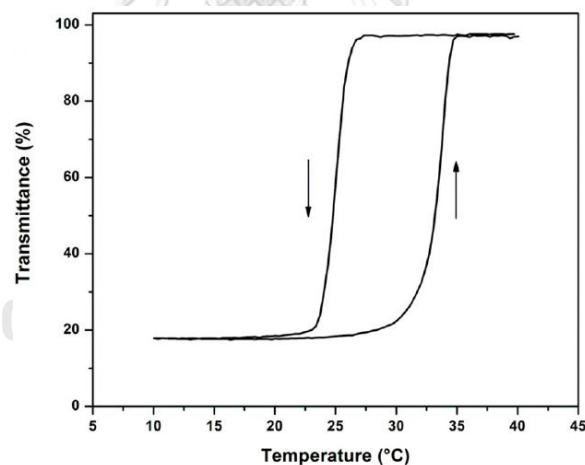


Figure 3.12 Optical transmittance as a function of temperature for a 200- μm thick film containing 30 wt.% C20 by heating/cooling cycle at 20°C/min.

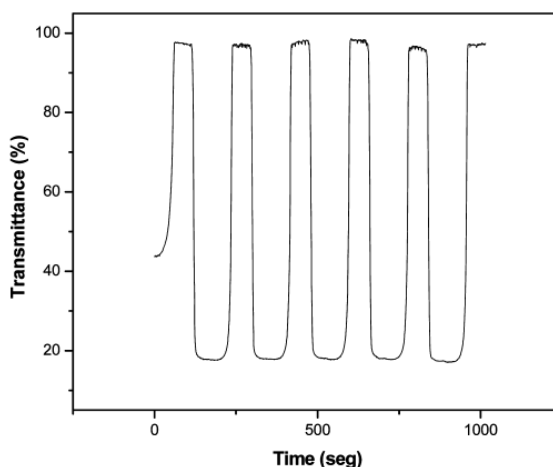


Figure 3.53 %Transmittance as a function of time during successive heating/cooling cycles at 20 °C/min for a 200- μ m thick TRLS film containing 30 wt.% C20.

S.Rimdusit, T.Mongkhonsi, P.Kamonchaivanich, K.Sujirote [37] studied effects of polyol molecular weight on properties of benzoxazine-urethane polymer alloys. From their result, the glass transition temperature of benzoxazine-urethane alloys increased with the increase of mass ratio urethane each polyol molecular weight (M_n). Furthermore, the observation of the thermal degradation of the BA:PU alloys at a fixed mass ratio of 80:20 did not increase at various molecular weights of the polyol. However, the char yields of these alloy systems were observed to increase with the molecular weights of the polyol. The char yields of the binary mixtures using PU1K, PU2K, PU3K, and PU5K were determined to be 18.3 wt.%, 20.6 wt.%, 22.6 wt.%, and 22.9 wt.%, respectively.

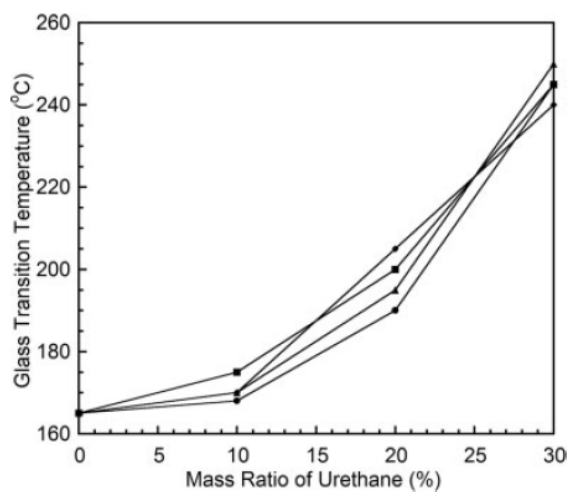


Figure 3.64 Relationship between M_n of polyol and glass transition temperature of BA:PU alloys from differential scanning calorimeter: (◆) $M_n = 1000$, (■) $M_n = 2000$, (▲) $M_n = 3000$, and (●) $M_n = 5000$ g/mol.

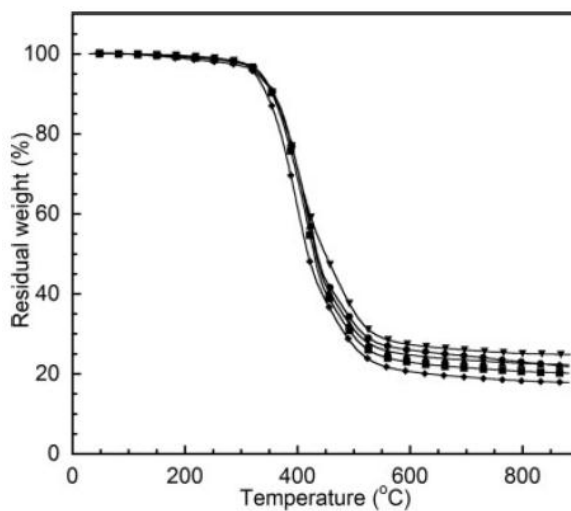


Figure 3.75 TGA thermograms of the BA:PU (80:20) polymer alloys at various number average molecular weights of polyol: (▼) Pure BA, (◆) $M_n = 1000$, (■) $M_n = 2000$, (▲) $M_n = 3000$, and (●) $M_n = 5000$ g/mol.

CHAPTER IV

EXPERIMENTAL

4.1 Raw Materials

Raw materials used in this research are benzoxazine resin and urethane prepolymer. Benzoxazine resin is based on bisphenol-A, paraformaldehyde and aniline. Bisphenol-A (polycarbonate grade) was supplied by PTT Phenol Co., Ltd. Paraformaldehyde (AR grade) was purchased from Merck. Aniline (AR grade) was obtained from Panreac Quimica SA Company. Urethane prepolymer was prepared by reacting polyether polyol with toluene diisocyanate (TDI). Toluene diisocyanate and poly(propylene glycol) with the number average molecular weights (M_n) of 1000, 2000, and 3000 g/mol was supported from IRPC Co., Ltd.

4.2 Specimen Preparation

4.2.1 Benzoxazine Resin Preparation

Benzoxazine monomer (BA) was synthesized by the patented solventless synthesis technique [38] from bisphenol A, paraformaldehyde, and aniline at the molar ratio 1:4:2. Briefly, the three reactants were continuously mixed in an aluminum pan at 110°C for 40 minutes. Subsequently, the reaction mixture was cooled-down to room temperature and the benzoxazine monomer (BA-a) was formed as a transparent yellowish solid. The product was then pulverized to fine powder and kept in a refrigerator for future-use.

4.2.2 Urethane Prepolymer Preparation

The urethane prepolymer was synthesized by mixing polypropylene glycol polyol ($M_w = 1000, 2000, \text{ or } 3000$) and 2,4-tolulene diisocyanate (TDI) at a 1:2 molar ratio in a four-necked round-bottomed flask. The mixture was then stirred under a nitrogen stream at 80°C for 2 hours without any addition of a catalyst. The obtained transparent and viscous urethane prepolymer was cooled down to room temperature and kept in refrigerator to prolong its shelf life. The urethane

prepolymers were labeled as PU1K, PU2K, and PU3K according to the M_n of the poly(propylene glycol) of 1000, 2000, and 3000 g/mol, respectively.

4.2.3 Benzoxazine:Urethane Prepolymer Binary Mixture Preparation

The benzoxazine monomer (BA-a) was mixed with PU1K, PU2K, and PU3K at a specified mass ratio (BA-a:PU) of 100:0, 90:10, 80:20, 70:30, 60:40, 50:50, and 60:40. The binary mixtures were sequentially heated at 130°C for 1 hour and at 150°C for 1 hour in an aluminium pan while thoroughly mixed until clear homogeneous resin mixtures were obtained. The molten resin was thermally cured in an air-circulated oven. The specimens were cured using a step heating profile at 160°C, 170°C, 180°C and 200°C for 2 hours at each temperature. The specimens were finally left to cool down to room temperature and were ready for the characterizations.

4.3 Characterizations

4.3.1 Attenuated Total Reflection Fourier Transform Infrared

Spectroscopy (ATR FT-IR)

A Nicolet iS5 FT-IR spectrometer (Thermo Scientific) equipped with fast recovery deuterated triglycine sulfate (DTGS) detector was employed for all infrared spectral acquisition. An iD5 single-bounce ATR accessories with a laminate-diamond

crystal was employed as a sampling probe. To acquire an infrared spectrum, the specimen surface was placed onto a flat diamond crystal IRE with sampling diameter of 1.5 mm. The specimen was pressed against the flat diamond crystal with a pressure device until the maximum allowable pressure was obtained. All ATR spectra were collected at 4 cm^{-1} with 32 co-addition scans.

4.3.2 Raman Spectroscopy

Raman spectra of all specimens were acquired with a DXR Raman Microscope (Thermo Scientific) with a 780-nm excitation laser. The specimens were analyzed under a 10X- objective lens with a laser spot size of $3.1\text{ }\mu\text{m}$. The laser power was set to 14.0 mW. A $50\text{-}\mu\text{m}$ slit type aperture was utilized for spectral acquisition. The exposure time for measuring was 2.0 seconds with 32 accumulated sample exposures. A 4th-degree polynomials was employed for spectral fluorescence correction. To obtain a Raman spectra, the tested specimen was mounted onto the sample stage beneath the objective lens. The spectral acquisition at a specified point was conducted by focusing the excitation laser on the surface. The surface of specimens should flat and smooth. The thickness of the specimen was 2 mm.

4.3.3 Optical Images and Optical Microscopy

The photographic images of BA-a/PU alloys were observed by a digital camera (IXUS 960 IS, CANON) with a resolution of 12.1 mega pixels. Optical micrographs in

reflection, transmission, and cross-polarized transmission modes of specimens were obtained with Axio Scope.A1 coupled with a AxioCam HRc CCD camera (Carl Zeiss).

4.3.4 Differential Scanning Calorimetry (DSC)

Differential scanning calorimeter model DSC1 Module (Mettler-Toledo) was used to study the curing behaviors of BA-a/PU mixtures. The samples with a mass in range of 5-10 mg were sealed in an aluminum pan with lid and were systematically scanned under nitrogen using a purging rate 50 mL/min. The sample was scanned from 30°C to 300°C at the heating rate of 10°C/min.

4.3.5 Light Scattering Apparatus

Thermo-optical properties of benzoxazine-urethane alloys were investigated with a homemade laser light scattering measurement apparatus. The insulator chamber had a dimension of 16 x 21 x 23cm³. In order to suppress a reflection of light, the interior wall of the test chamber was coated with black color. The chamber contains a heater, a multimeter, a temperature controller set, a type K thermocouple, a BPW21 visible light Si photodiode, and a laser source. The heating temperature up to 300°C can be precisely controlled. The laser generated from the laser source had a wavelength within the range from 630 nm to 680 nm. The dynamic range of the photodiode was 460–750 nm.

4.3.6 Dynamic Mechanical Analysis (DMA)

The dynamic mechanical analyzer (DMA) model DMA242 from NETZSCH was employed to investigate the thermomechanical properties of the specimens. The dimension of each specimen was 50 × 10 × 2 mm. The test was performed under the three-point bending mode. The temperature was scanned from -100°C to the temperature beyond the glass transition temperature (T_g) of each specimen with a heating rate of 2°C/min under nitrogen atmosphere. The strain was applied sinusoidally with a frequency of 1 Hz. The storage modulus (G'), loss modulus (G''), and loss tangent ($\tan \delta$) were then obtained. The glass transition temperature was obtained from the local maxima on the loss modulus or the loss tangent curves.

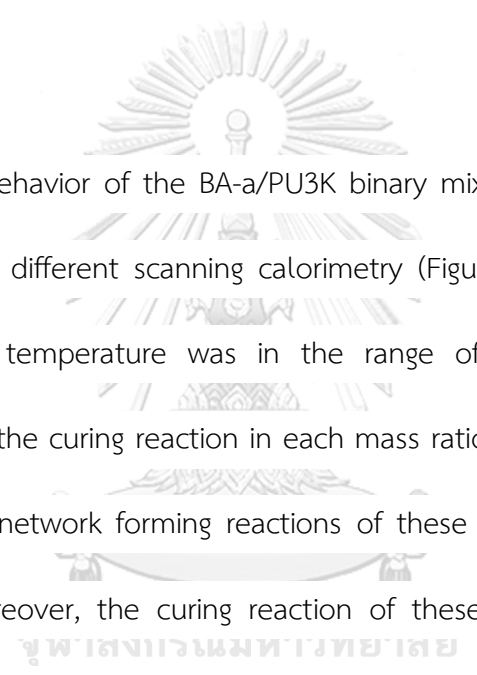
4.3.7 Thermogravimetric Analysis (TGA)

Thermal stability of benzoxazine-urethane samples was performed on a Mettler Toledo thermogravimetric analyzer model TGA1 STAR^e System. The testing temperature program was ramped at a heating rate of 20°C/min from 30°C to 800°C under nitrogen atmosphere with a constant N₂ purging at a flow rate of 50 mL/min. The sample mass was approximately 5-10 mg. The degradation temperature at 5% weight loss ($T_{d,5}$) and char yield at 800°C were recorded for each specimen.

CHAPTER V

RESULTS AND DISCUSSION

5.1 Differential scanning calorimetry for curing condition observation



The curing behavior of the BA-a/PU3K binary mixtures at various mass ratio was investigated by differential scanning calorimetry (Figure 5.1). A heating rate was $10^{\circ}\text{C}/\text{min}$ and the temperature was in the range of $30\text{--}300^{\circ}\text{C}$. Only a single exothermic peak of the curing reaction in each mass ratio was observed. The results suggested that the network forming reactions of these binary mixtures took place simultaneously. Moreover, the curing reaction of these binary system proceeded without the need of any catalyst or curing agent. The exothermic peak was shifted to higher temperature when PU3K content increased. When the mass ratio of BA-a/PU3K resin mixtures was 100/0, 90/10, 80/20, 70/30, 60/40, 50/50, and 40/60, the exothermic peak was at 233, 238, 243, 247, 253, 256 and 262°C respectively. The curing retardation was attributed to the dilution effect of the urethane prepolymer [20]. Takeichi et al. reported that initially phenolic hydroxyl group from the ring opening of the benzoxazine monomer was produced after that the reaction between

phenolic hydroxyl group on the polybenzoxazine and the isocyanate group was expected to proceed [19]. The DSC thermogram also showed the decrease of curing peak area of the binary mixtures when the amount of the PU resin increased. The systematic decrease of the exotherms with the PU revealed that the BA:PU interaction possessed a lower heat of reaction per mole of the reactant than that of the BA:BA interaction. Excessive amount of the PU in the binary mixtures might also lead to the presence of the unreacted PU in the fully cured alloys [37].

Since the BA-a/PU3K alloy at a mass ratio of 40:60 exhibited the highest curing temperature, the alloy was selected in order to determine the fully-cured condition for other binary mixture compositions. The DSC thermograms of BA-a/PU3K alloy at various curing conditions are shown in Figure 5.2. The degree of conversion of the sample was calculated by the following relationship.

$$\% \text{ conversion} = \left(1 - \frac{H_{rxn}}{H_0}\right) \times 100$$

where H_{rxn} is a heat of reaction of a partially cured specimen.

H_0 is a heat of reaction an uncured resin.

Both H_{rxn} and H_0 values can be obtained from DSC experiment.

The fully-cured condition of the polymer corresponded to the complete disappearance of the exothermic peak in DSC thermograms. Theoretically, the fully - cured polymer was reported to provide a polymer with high thermal and mechanical properties. The heat of reaction determined from the area under the exothermic peak was 105.45 J/g (0% conversion) for the uncured 40:60 of BA-a/PU3K alloys. The heat of reaction reduced to 82.75 J/g (21% conversion), 79.43 J/g (24% conversion) and 64.17 J/g (39% conversion) after the thermal curing at 130°C for 1 hour, 150°C for 1 hour, 160°C for 2 hour, respectively. The heat of reaction decreased to 26.32 J/g (75% conversion) after further thermal curing at 170°C for 2 hour. When the binary mixture was cured at 180°C for 2 hour, the heat of reaction decreased to 10.05 J/g (90% conversion). The exothermic heat of reaction disappeared after post-curing at 200°C for another 2 hours. The results suggested that the curing reaction of BA-a/PU3K alloys could rapidly occur at temperature above 130°C. The curing reaction was complete after the binary mixture was cured at 200°C for 2 hours. Therefore, the step-curing conditions starting from 130°C for 1 hour, 150°C for 1 hour, 160°C for 2 hours, 170°C for 2 hours, 180°C for 2 hours, and 200°C for 2 hours was chosen as an optimum curing condition for all BA-a/PU3K binary mixtures.

5.2 Optical Images

The inherent transparency of polybenzoxazine and BA-a/PU alloys at room temperature are shown in Table 5.1. The dimensions of all specimens were 12 x 40 x 2 mm. BA-a/PU2K alloys with PU2K mass fractions of 30% and 40% and BA-a/PU3K alloys with PU3K mass fractions of 30%, 40%, and 50% exhibited the opaque state at room temperature. On the other hand, BA-a/PU1K alloys with PU1K mass fractions from 30–60%, BA-a/PU2K alloys with PU2K mass fractions of 10%, 50%, and 60%, and BA-a/PU3K alloys with PU3K mass fractions of 10% and 60% displayed the transparent state. The semi-transparent state was observed in BA-a/PU1K alloys with PU1K mass fractions of 10% and 20%, BA-a/PU2K alloys with PU2K mass fraction of 20%, and BA-a/PU3K alloys with PU3K mass fraction of 20%. Therefore, the addition of PU2K and PU3K into polybenzoxazine can induce the opaque state in BA-a/PU alloys. Moreover, the molecular weights of polyol greatly affected the inherent transparency of BA-a/PU alloys. BA-a/PU alloys fabricated from PU3K prepolymer exhibited the broader range of the opaque state compared to BA-a/PU alloys fabricated from PU2K prepolymer with the same mass fraction from 30–50%. Interestingly, BA-a/PU2K alloys with PU2K mass fraction of 30%, which was in the opaque state at room temperature, shifted to the transparent state at 200°C (Figure 5.3).

5.3 Optical Microscopy

In order to observe the morphology and optical properties of the polymers, polyurethane, polybenzoxazine, and PU3K/BA-a alloys with PU3K mass fractions of 30% and 60% were fabricated to 100- μm thick films. Glass slides were employed as substrates for all specimens. Polyurethane and polybenzoxazine films transmitted the visible light (Figure 5.4). However, when the polarized light was employed, both polyurethane and polybenzoxazine did not exhibit any optical activity. Similarly, 60wt% PU/BA-a alloy films which were transparent, did not distort the plane-polarized light and optical micrographs exhibiting only dark area were observed.

In contrast, 30wt% PU/BA-a alloy films displayed some optical activity with the plane-polarized light. Visible light cannot transmit through the films. Moreover, the films appeared opaque when observed with the naked eyes. When we closely investigated the optical micrographs in cross-polarized transmission modes of 30wt% PU3K/BA-a alloys (Figure 5.5), we observed that the dense polymeric matrix were gradually built up from many micrometer-sized domains. These small polymeric microdomains were formed by the crosslinking between BA-a resin and urethane prepolymer during the sequential step curing from 130–200°C. Visible light was scattered by the micrometer-sized domains of PU-crosslinked polybenzoxazine since dark area where these microdomains were located was observed. The magnitude of the light scattering depended on the local concentration of the microdomains as

observed from the optical micrographs in the transmission mode. These polymeric microdomains were capable of distorting the plane-polarized light. In addition, we can clearly observe the distribution of the polymeric microdomains from the optical micrographs where the cross-polarized light was employed. The inhomogeneity in the distribution of these polymeric microdomains was one of the cause of the light scattering observed in our system. When the PU content in PU3K/BA-a alloys increased to 60wt%, the size of the polymeric microdomains was smaller than wavelengths of the visible light. The light scattering in 60wt% PU3K/BA-a alloys was not observed at room temperature.

The bulk refractive indices of PU3K prepolymer, PU3K polymer, and BA-a/PU3K alloys with PU3K mass fraction of 60%, and polybenzoxazine were 1.4645, 1.4672, 1.54, and 1.671 respectively. The refractive index of benzoxazine-urethane alloys at room temperature laid between the values of polybenzoxazine and polyurethane. There was a refractive index mismatch in the alloys at the opaque state. In addition, the light scattering state of the alloys were caused by phase-separated nonuniform distribution of segregated PU in PU-crosslinked polybenzoxazine alloy. At the elevated temperature that was higher than the transition temperature, the bulk refractive indices of PU and benzoxazine were reduced and converged to the specific value. The transparent state of the alloy was obtained when there was a perfect refractive index matching for both PU and polybenzoxazine.

5.4 Light scattering apparatus

The thermo-optical curves of BA-a/PU2K alloys with PU2K mass fractions of 30% and 40% are shown in Figure 5.6 and Figure 5.7, respectively. The thermo-optical curves of BA-a/PU3K alloys with PU3K mass fractions of 30%, 40% and 50% are shown in Figure 5.8, Figure 5.9, and Figure 5.10, respectively. The transition temperatures of heating and cooling step were determined from the midpoint of the optical state transition in thermo-optical curves of each BA-a/PU2K and BA-a/PU3K alloy specimen. The transition temperature decreased from 84°C to 67°C in the heating step and 73°C to 63°C in the cooling step when PU2K mass fraction of BA-a/PU2K alloys increased from 30% to 40%, respectively (Table 5.2). In BA-a/PU3K alloys, the transition temperatures in the heating step were decreased from 128°C to 104°C when PU3K mass fractions increased from 30% to 50% in Figure 5.8, Figure 5.9 and Figure 5.10. The thermally reversible light scattering behavior is attributed to the fact that at elevated temperature, the refractive indices of BA-a/PU and PU are converged to the same value. The optical inhomogeneity in the specimen was minimized, and in turn, the light scattering process in the specimen was attenuated. The refractive index of PU might be more sensitive to temperature change than that of BA-a/PU. When PU mass fraction increased, the switching temperature of the alloys decreased. In contrast, when PU2K mass fraction in BA-a/PU2K alloy was 50%,

the alloy were transparent for all temperature range, suggesting the miscible nature of the alloy.

5.5 ATR FT-IR and Raman Spectra

ATR FT-IR spectra and Raman spectra of BA-a resin, polybenzoxazine, PU3K prepolymer, and BA-a/PU3K alloys at various PU3K mass fractions are shown in Figure 5.11. The infrared absorption peaks of BA-a resin at 942 cm^{-1} and 1229 cm^{-1} were attributed to the benzene mode of the benzene ring that is adjacent to the oxazine ring and the trisubstituted benzene of the oxazine ring, respectively [20]. The infrared absorption peaks at 1599 cm^{-1} and the Raman shift at 1600 cm^{-1} of BA-a resin were assigned to the benzene ring C=C stretching vibrations [39], [40]. The Raman shift at 3063 cm^{-1} and the infrared band in the region from $2990\text{--}3110\text{ cm}^{-1}$ came from the aromatic =C-H stretching vibrations of BA-a resin. The Raman shift at 2969 cm^{-1} and the infrared absorption peak at 2964 cm^{-1} of BA-a resin were attributed to the methyl C-H stretching vibrations. Alkane C-H deformations from the $-\text{C}(\text{CH}_3)_2$ functional group of BA-a were exhibited in the infrared absorption peak at 1382 cm^{-1} and 1362 cm^{-1} and the Raman band centered at 1372 cm^{-1} . The infrared absorption peak and the Raman shift of BA-a at 1156 cm^{-1} were assigned to C-C skeletal vibrations of $-\text{C}(\text{CH}_3)_2$. Tertiary aromatic amines from oxazine ring of BA-a resin showed C-N stretching vibrations at 1302 cm^{-1} in the Raman spectrum and at 1325

cm^{-1} in the infrared spectra. The Raman shift of BA-a at 1031 cm^{-1} and the infrared absorption peak at 1029 cm^{-1} of BA-a resin were attributed to the symmetric C–O–C stretching from the benzoxazine ring. Polybenzoxazine was formed from BA-a resin by thermal-triggered ring-opening polymerization [41]. Benzoxazine monomers were transformed from a ring structure to a nearly infinite three-dimensional network. The C–O–C stretching peak was disappeared in the Raman spectra of polybenzoxazine because the oxazine ring in BA-a resin was opened by the breakage of a C–O bonds. In addition, broad infrared absorption band situated around 3367 cm^{-1} was observed in the polybenzoxazine spectra due to the in situ generated phenolic hydroxyl groups from the polymerization process. The combination of deformation vibrations of hydroxyl groups and C–O stretching vibrations was observed at 1176 cm^{-1} in the infrared spectra of polybenzoxazine. This intense peak was not observed in the infrared spectra of BA-a resin. Trisubstituted benzene ring in BA-a resin was transformed into 1,2,3,5-tetrasubstituted benzene ring in polybenzoxazine after the polymerization. This transformation was confirmed by the disappearance of the infrared absorption peaks at 942 and 1229 cm^{-1} in polybenzoxazine spectra.

In Situ generated hydroxyl groups during the thermal curing of BA-a resin can be employed for the crosslinking with urethane prepolymer to generate BA-a/PU alloys. Urethane prepolymer was prepared from by reacting poly(propylene glycol) and toluene diisocyanate at the molar ratio of 1:2 under a nitrogen atmosphere. The intense infrared absorption peaks at 2970 and 2867 cm^{-1} and the

Raman shifts at 2974 and 2871 cm^{-1} in the PU3K spectra were attributed to the asymmetric C–H stretching and symmetric C–H stretching of aliphatic methyl groups, respectively. Acyclic symmetric $-\text{CH}_2-$ stretching vibrations were observed at 2930 cm^{-1} in the infrared spectra and at 2932 cm^{-1} in the Raman shift of PU3K spectra. An ether C–O stretching vibration of $-\text{CH}_2-\text{O}-\text{CH}_2-$ was observed at 1092 cm^{-1} as the intense peak in the infrared spectra of PU3K. PU3K was terminated with free isocyanate groups because the intense infrared absorption peak attributed to the asymmetric aryl isocyanate ($-\text{N}=\text{C}=\text{O}$) stretching vibrations was observed at 2272 cm^{-1} . BA-a resin and urethane prepolymer can be alloyed through the formation of urethane linkage ($-\text{NH}-\text{CO}-\text{O}-$). The terminal isocyanate groups in urethane prepolymer were reacted with in situ generated hydroxyl groups of BA-a during thermal ring-opening polymerization. The complete disappearance of the peak at 2272 cm^{-1} of the infrared spectra of BA-a/PU3K alloys with PU3K mass fraction of 30% and 60% indicated that isocyanate groups in PU3K were completely consumed during the alloy formation process. Urethane C=O stretching vibrations (Amide I band) of solid phase *N*-aryl urethanes of BA-a/PU3K with PU3K mass fraction of 30% and 60% were observed at 1705 cm^{-1} and 1709 cm^{-1} in the infrared spectra, respectively. ATR FT-IR spectra and Raman spectra of BA-a/PU3K alloys were greatly resembled the vibrational characteristics of both polybenzoxazine and urethane prepolymer. These results indicated that BA-a and PU3k prepolymer were alloyed

through the formation of the urethane linkage under the step curing employed in our fabrication.

5.6 Dynamics Mechanical Analysis (DMA)

The mechanical properties of BA-a/PU3K alloys were investigated by a dynamic mechanical analyzer (DMA). The experiment was performed under a flexural mode from -100°C to 350°C. The dynamic mechanical properties of the BA-a/PU3K alloys at the PU3K mass fractions of 0%, 30%, 40%, and 50% are shown in Figure 5.12. The storage modulus of alloys at their glassy state tended to decrease with increasing PU mass fractions. The storage modulus at room temperature of the neat polybenzoxazine and the polyurethane were determined to be 6,627 MPa and 44 MPa, respectively. BA-a/PU3K alloys exhibited the storage modulus at room temperature of 1,857 MPa, 1,546 MPa, and 1,066 MPa at the BA-a/PU3K mass ratio of 70/30, 60/40, and 50/50, respectively. This result indicated that the addition PU in the polymer alloys made the materials more flexible. When benzoxazine was a major component, rubbery plateau modulus of polymer alloys was increased with urethane prepolymer mass fraction. Crosslink density of a polymer network can be calculated from rubbery plateau modulus as suggested by Nielsen [42].

$$\log\left(\frac{E'}{3}\right) = 7.0 + 293\rho_x \quad (5.1)$$

E' is a storage modulus in a rubbery plateau region (dyn/cm^2), ρ_x is a crosslinked density defined as the mole of network chains per unit volume of the polymers (mol/cm^3). The crosslinked densities of all polymer alloys that determined from the equation 5.1 were found to increase with the mass fraction of the urethane prepolymer.

The glass transition temperature (T_g) of BA-a/PU3K alloy was determined from the peak maximum of the loss modulus (E'') curves (Figure 5.13). T_g depends largely on molecular structure (steric effect), chain flexibility, branching and crosslinking, and molar mass [43]. The T_g of the neat polybenzoxazine was determined to be 160°C . The BA-a/PU3K alloys showed two peak maxima or two T_g in loss modulus curve. The peak at -68°C was attributed to the polyurethane domain in the alloys. Another peak at higher temperature was a T_g of BA-a/PU3K alloys. The T_g of the polymer alloys were about 258°C , 268°C , and 284°C when the mass ratio of BA-a/PU3K were 70/30, 60/40, and 50/50, respectively. This suggested that BA-a/PU3K alloys were a heterogeneous network that composed of polyurethane domain and urethane-benzoxazine domain. Increasing urethane elastomer into polybenzoxazine can substantially increase the T_g of the polymer alloys. Moreover, the synergistic behavior of the T_g of the alloys was observed since the T_g of all investigated alloys were greater than the T_g of both the polybenzoxazine and polyurethane. The glass transition temperature and network of BA-a/PU3K alloys were also examined in loss tangent ($\tan \delta$) curves (Figure 5.14). The $\tan \delta$ or loss tangent curves were obtained

from the ratio of energy loss or viscous part (E'') to storage energy or elastic part (E') of dynamic modulus of material. The T_g of the polymer alloys can also be determined from the local maxima on the $\tan \delta$ curve of each specimen. The T_g 's of the alloys were shifted to higher temperature when the urethane prepolymer mass fraction in the alloys increased. Moreover, the magnitude of the $\tan \delta$ peak reflects the large scale mobility associated with alpha relaxation. The peak height of the local maxima in $\tan \delta$ curves tended to decrease when the mass fraction of the urethane prepolymer increased. This suggested the reduction in the chain's segmental mobility due to the increasing crosslinked density. Furthermore, the width at half height of the local maxima in $\tan \delta$ curves were corresponded to the network heterogeneity of the system. Specifically, the width at half heights of the $\tan \delta$ curves for BA-a/PU3K alloys were broader when urethane prepolymer mass fraction in the polymer alloys increased. Therefore, urethane prepolymer induced the formation of nonhomogeneous network in the polymer alloys.

5.7 Thermal Degradation and Thermal Stability Investigation

The TGA thermograms of the polybenzoxazine and BA-a/PU3K alloys at various PU3K mass fractions are shown in Figure 5.15 The degradation temperature of the neat polybenzoxazine at 5% weight loss ($T_{d,5}$) was determined to be 334°C. The $T_{d,5}$ of BA-a/PU3K at PU3K mass fractions of 30%, 40%, and 50% were determined to

be 355°C, 365°C and 374°C, respectively. Incorporation of the urethane resin into the benzoxazine resin raised the thermal degradation temperature of the obtained alloys. Therefore, the thermal stability of the polybenzoxazine was improved. The enhanced thermal stability are, in part, due to the relatively more stable chemical bonds in the polyether polyol in contrast to a polybenzoxazine network containing less stable Mannich bridge. The char yield, which is residual weight at 800°C, of the neat polybenzoxazine was determined to be 27wt%. When the PU3K mass fractions in the alloys were 30%, 40%, and 50%, the char yield were found to be 23.5wt%, 22.9wt% and 21wt%, respectively. The residual weight of the BA-a/PU3K alloys decreased when PU3K mass fraction increased. This result comes from the fact that the chemical structure of the polyurethane composes of a less char forming aliphatic structure of the polypropylene glycol compared to the prevalent aromatic benzene rings in the network structure of the polybenzoxazine [18],[19],[20].

CHAPTER VI

CONCLUSIONS

Benzoxazine-urethane polymer alloys exhibiting thermally reversible light scattering properties were successfully fabricated. When BA-a/PU2K 30–40wt% alloys and BA-a/PU3K 30–50wt% alloys were exposed to heat from room temperature to 140°C, these alloys exhibited the light scattering state to transparent state transition with the transition temperatures of 84–67°C and 128–104°C, respectively, depending on the PU mass fractions. When the alloy specimens were cooled down to room temperature, they were reversibly transformed to the opaque state again with the transition temperatures of 73–63°C for BA-a/PU2K alloys at the PU2K contents of 30–40wt% and 114–82°C for BA-a/PU3K alloys at the PU3K contents 30–50wt%. Urethane prepolymer and benzoxazine monomers were covalently crosslinked through the urethane linkage. Some fractions of PU were phase-separated from PU-crosslinked polybenzoxazine as observed in the loss tangent curves of BA-a/PU alloys. The two phase observed as the peak maxima in the loss tangent curve were PU and BA-a/PU copolymer. PU-crosslinked polybenzoxazine exhibited the morphologies of micrometer-sized polymeric domains. The size of microdomains depended on the PU mass fractions and the PU molecular weights. The micrometer-sized domains caused by the microphase separation were observed in the 100- μm thick specimen

of the BA-a/PU alloy at the PU content of 30wt% by the polarization microscope. The microphase separation, the refractive index matching, and the micrometer-sized domains of PU-crosslinked polybenzoxazine played important roles as the determining factor for the optical state of the BA-a/PU alloys. Benzoxazine-urethane polymer alloys showed synergistic behaviors in glass transition temperatures and thermal stability when the PU mass fractions in the alloys increased. Our developed materials were suitable for employing in opto-thermal sensing applications.



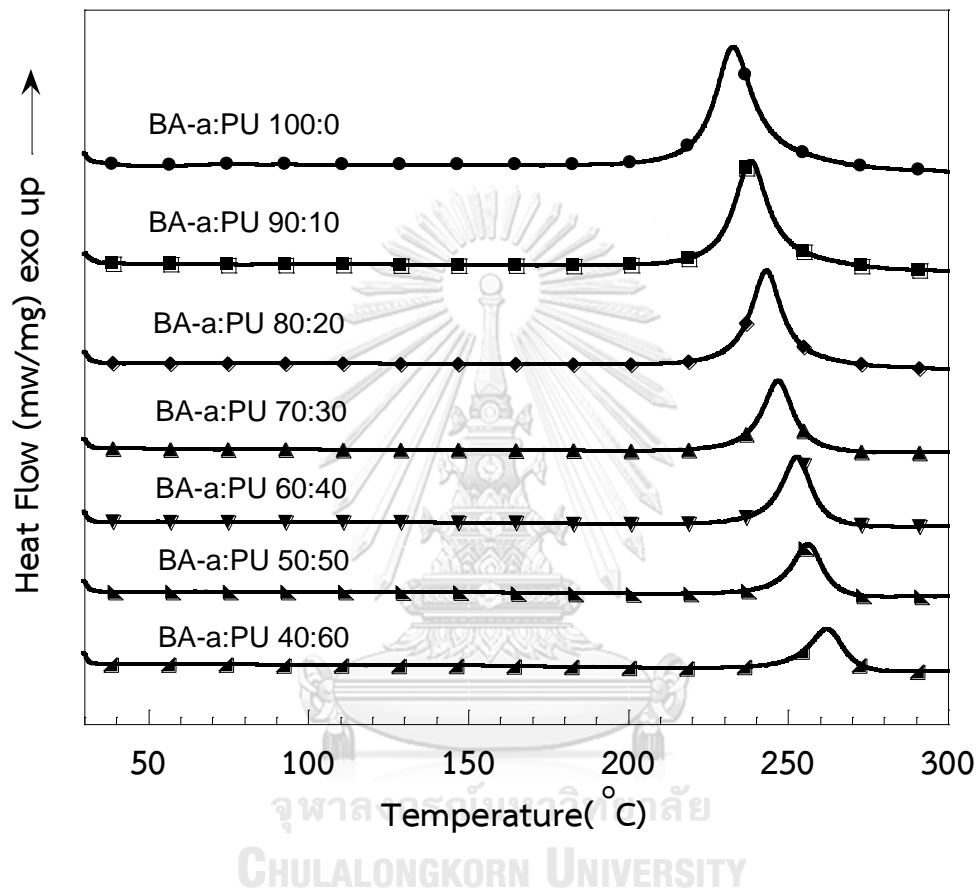


Figure 5.1 DSC thermograms of benzoxazine-urethane resin mixtures at various BA-a:PU3K mass ratios: (●)100:0, (■)90:10, (◆)80:20, (▲)70:30, (▼)60:40, (▴)50:50, and (◄)40:60.

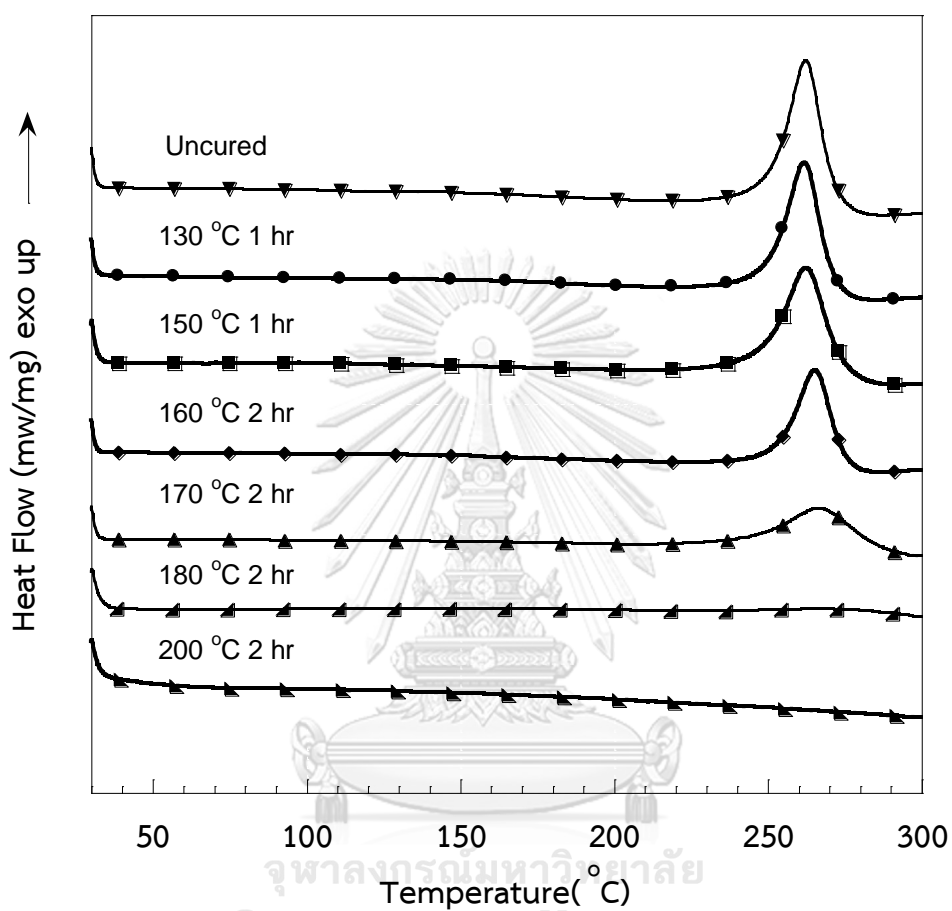











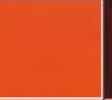






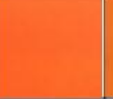




Figure 5.2 DSC thermograms of benzoxazine-urethane resin mixtures at 40:60 mass ratio at various curing conditions: (▼)Uncured, (●)130 °C 1hr, (■)150 °C 1hr, (◆)160 °C 2hr, (▲)170 °C 2hr, (▲)180 °C 2hr, and (▲)200 °C 2hr.

Table 5.1 Visual appearance of BA-a/PU alloys at room temperature.

Molecular weight of polyol	PU content (%)						
	0wt%	10 wt%	20 wt%	30 wt%	40 wt%	50 wt%	60wt%
MW 1000							
MW 2000							
MW 3000							

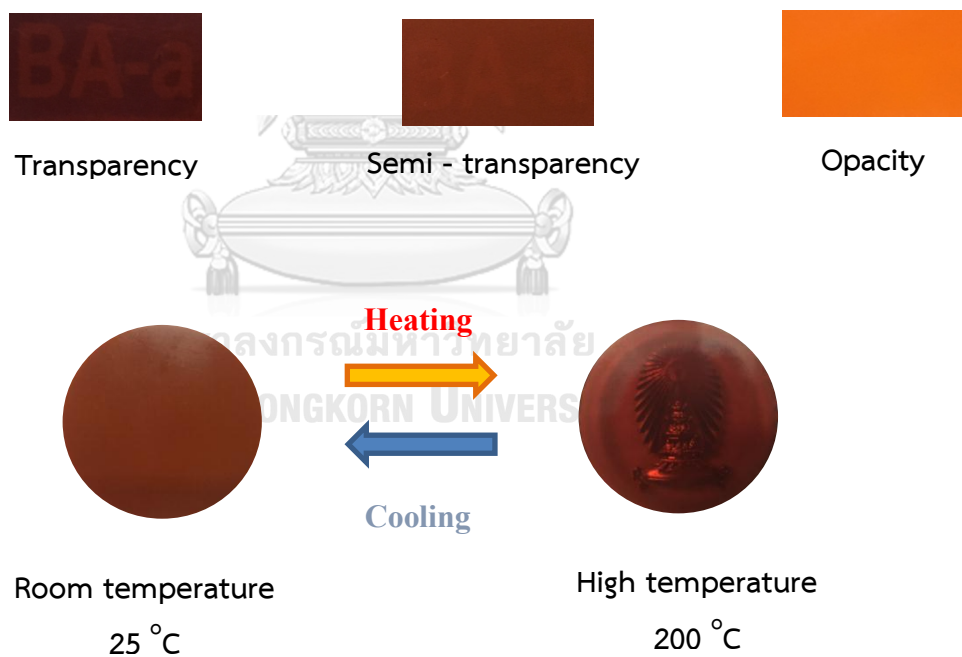


Figure 5.3 Thermally reversible light scattering behaviors of BA-a/PU2K.

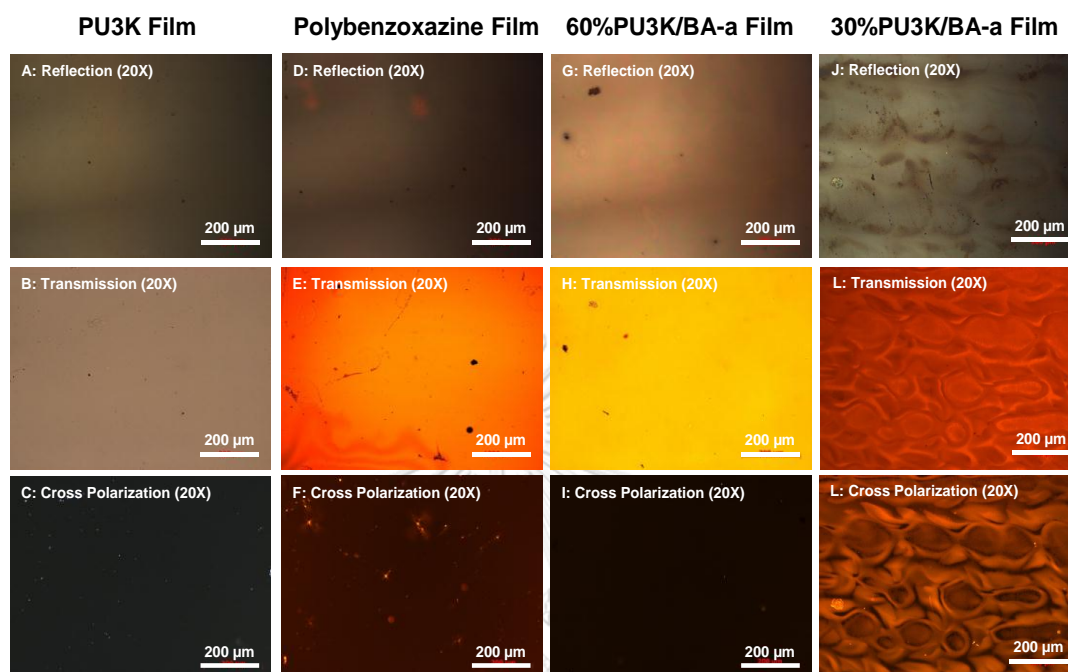


Figure 5.4 Optical micrographs of 100- μm thick PU3K (A–C), polybenzoxazine (D–F), 60%PU3K/BA-a (G–I), and 30%PU3K/BA-a films in reflection, transmission, and cross-polarized transmission modes. The magnifications of all micrographs are 20X. The

scale bars in all micrographs are 200 μm .

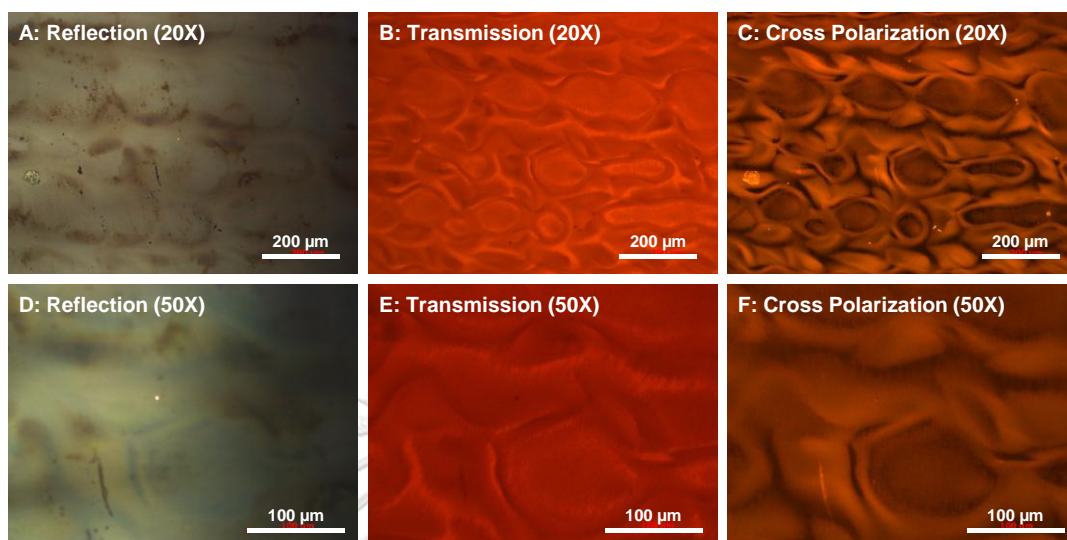


Figure 5.5 Optical micrographs of 100- μm thick 30%PU3K/BA-a films in reflection (A and D), transmission (B and E), and cross-polarized transmission (C and F) modes. The magnifications of the micrographs are 20X (A–C) and 50X (D–F). The scale bars in A–C and D–F are 200 μm and 100 μm , respectively.

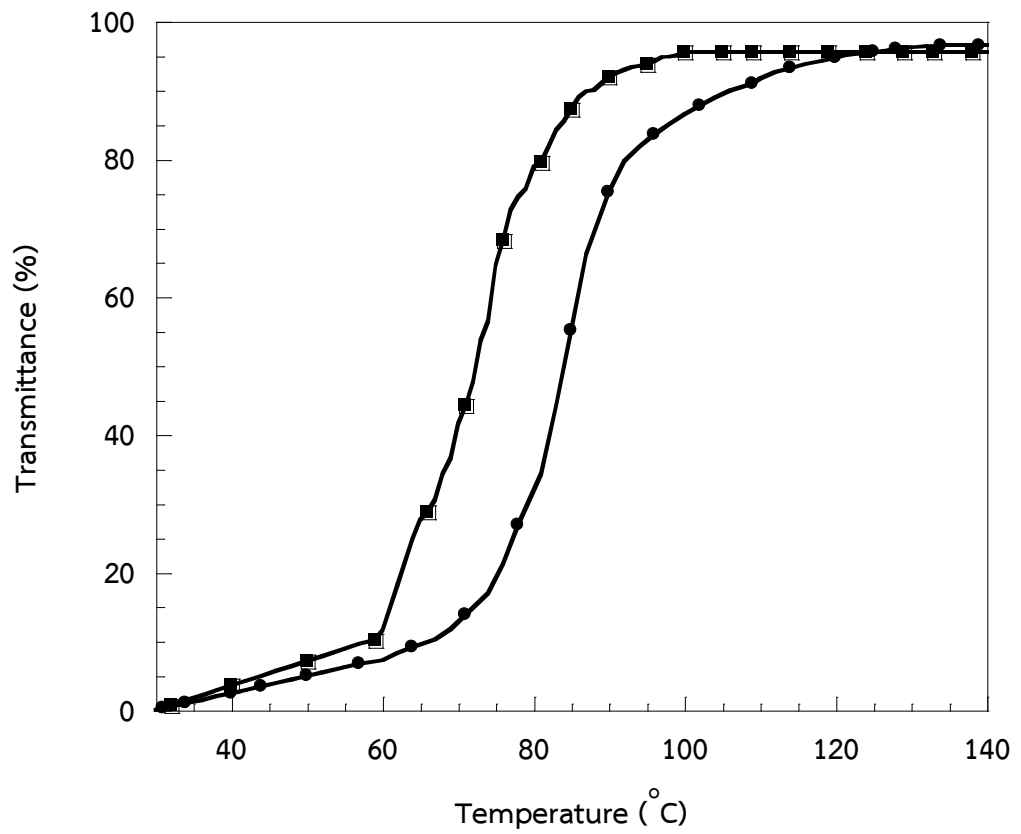


Figure 5.6 Thermo-optical curve of BA-a/PU2K alloys at 30wt%:

(●) Heating and (■) Cooling

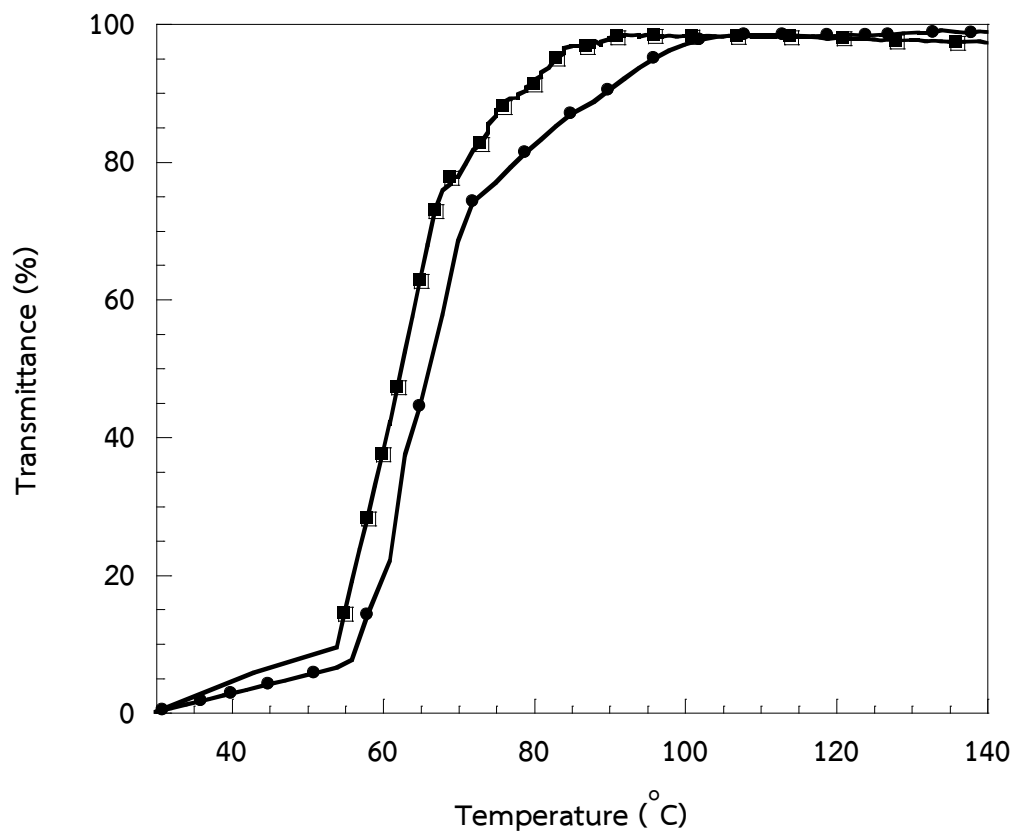


Figure 5.7 Thermo-optical curve of BA-a/PU2K alloys at 40wt%:

(●) Heating and (■) Cooling

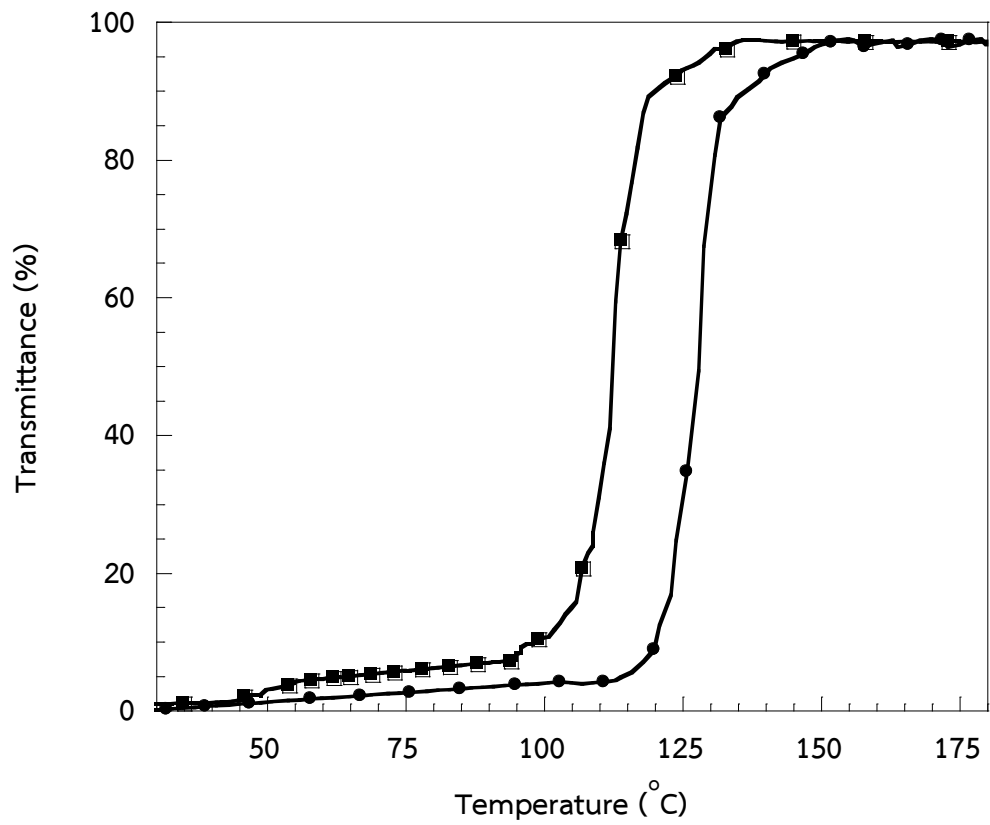


Figure 5.8 Thermo-optical curve of BA-a/PU3K alloys at 30wt%:

(●) Heating and (■) Cooling

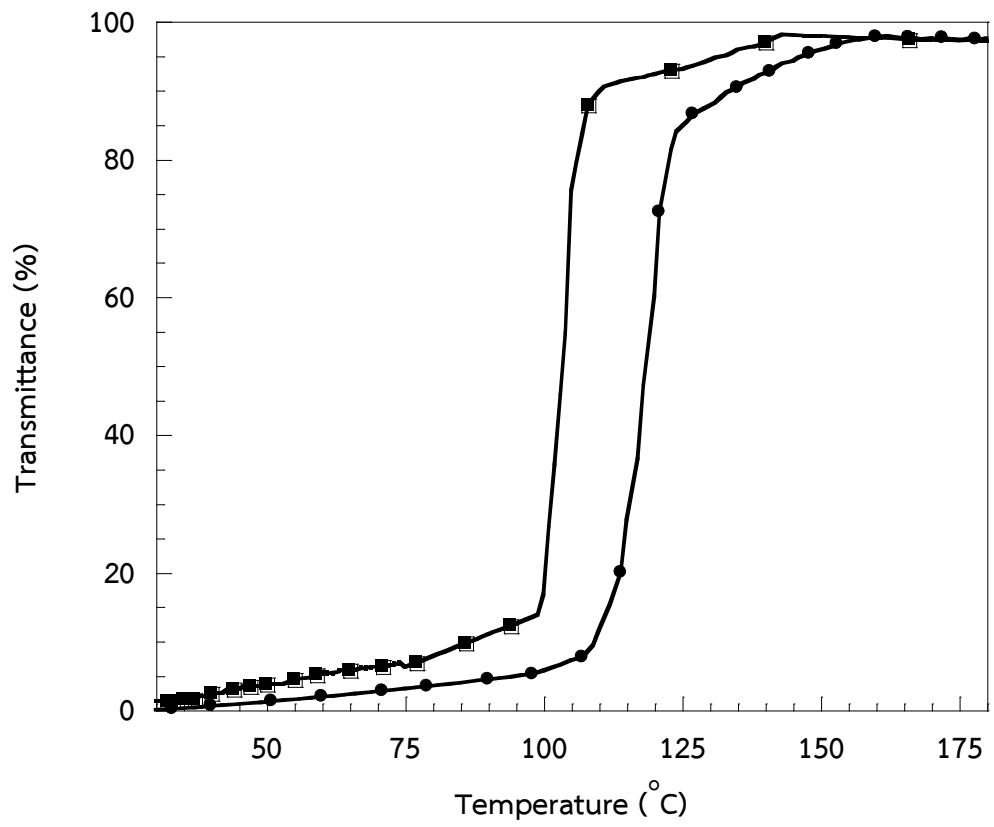


Figure 5.9 Thermo-optical curve of BA-a/PU3K alloys at 40wt%:

CHULA (●) Heating and (■) Cooling

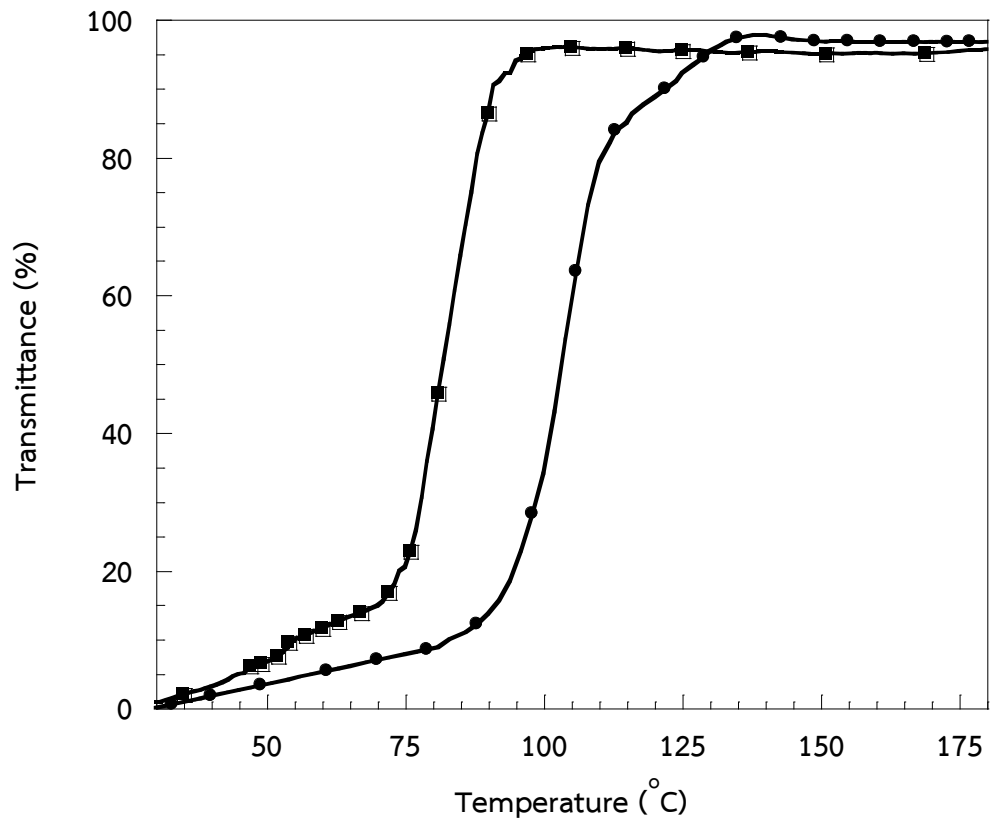


Figure 5.10 Thermo-optical curve of BA-a/PU3K alloys at 50wt%:

(●) Heating and (■) Cooling

Table 5.2 Transition temperature of BA-a/PU2K and BA-a/PU3K at various alloy mass ratios.

Molecular weight of polyol	PU content (wt%)	Transition temperature of heating step (°C)	Transition temperature of cooling step (°C)
MW 3000	30	128	114
	40	119	104
	50	104	82
MW 2000	30	84	73
	40	67	63
	50	Transparent for all temperature range	

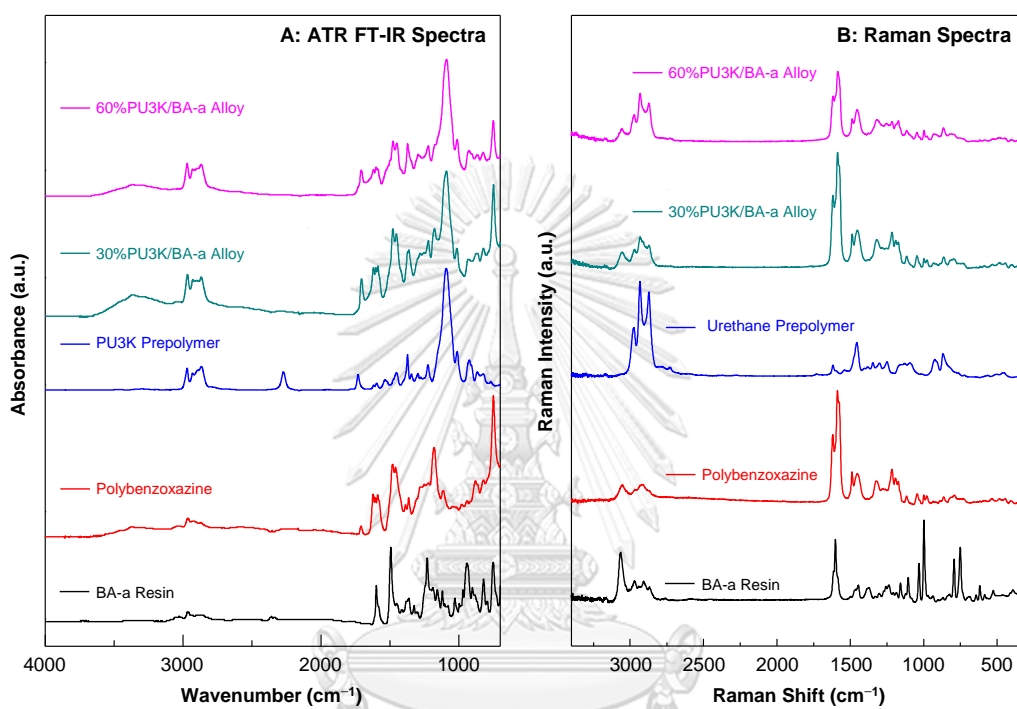


Figure 5.11 ATR FT-IR spectra (A) and Raman spectra (B) of BA-a resin, polybenzoxazine, PU3K prepolymer, and BA-a/PU3K alloys at various PU3K mass fractions.

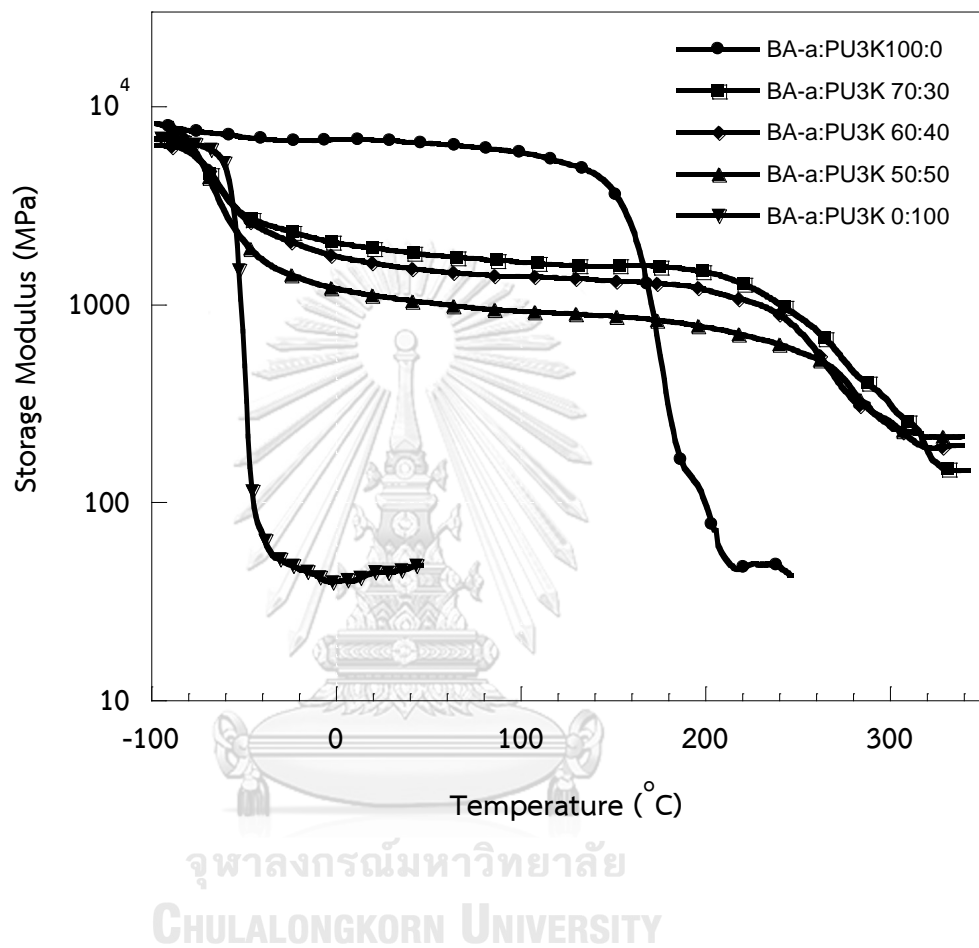


Figure 5.12 Storage modulus of BA-a:PU3K copolymers at various mass ratios:

(●)100:0, (■)70:30, (◆)60:40, (▲)50:50 and (▼)0:100

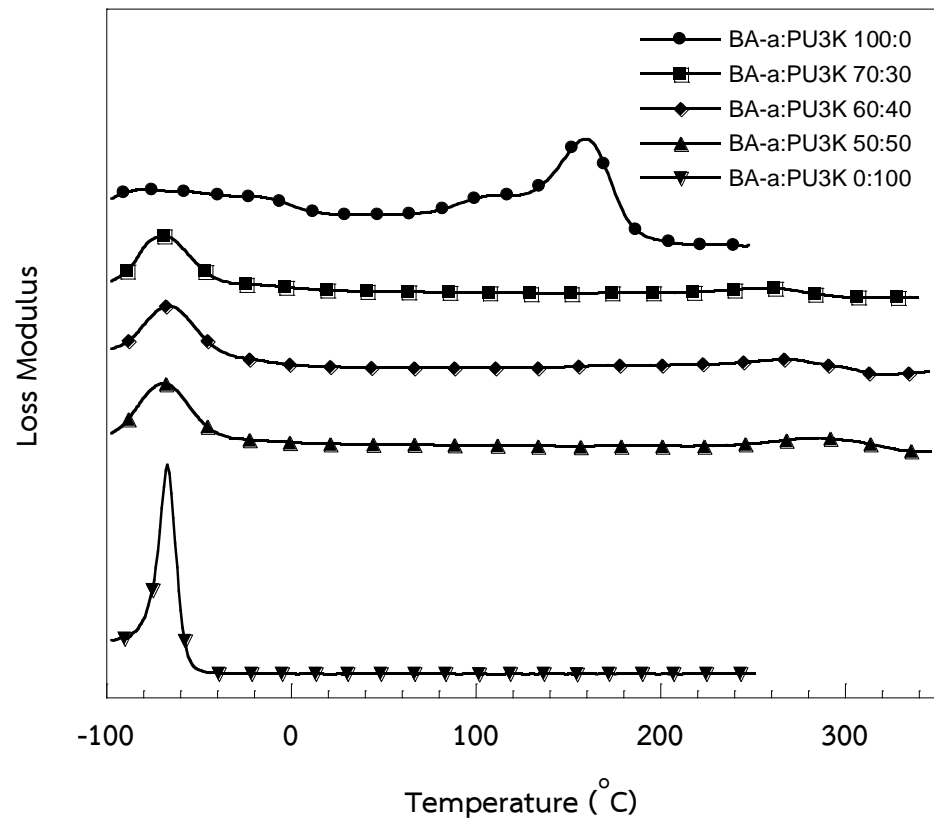


Figure 5.13 Loss modulus of BA-a:PU3K copolymers at various mass ratios:

(●)100:0, (■)70:30, (◆)60:40, (▲)50:50 and (▼)0:100

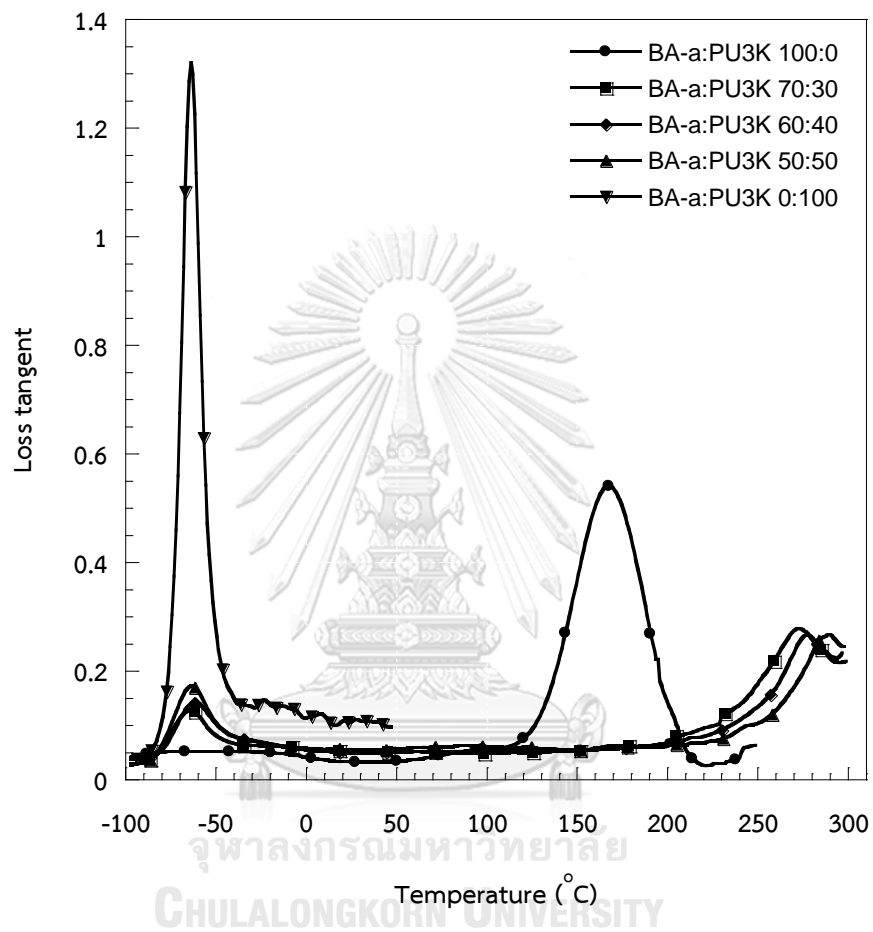


Figure 5.14 Loss tangent of BA-a:PU3K copolymers at various mass ratios:

(●)100:0, (■)70:30, (◆)60:40, (▲)50:50 and (▼)0:100

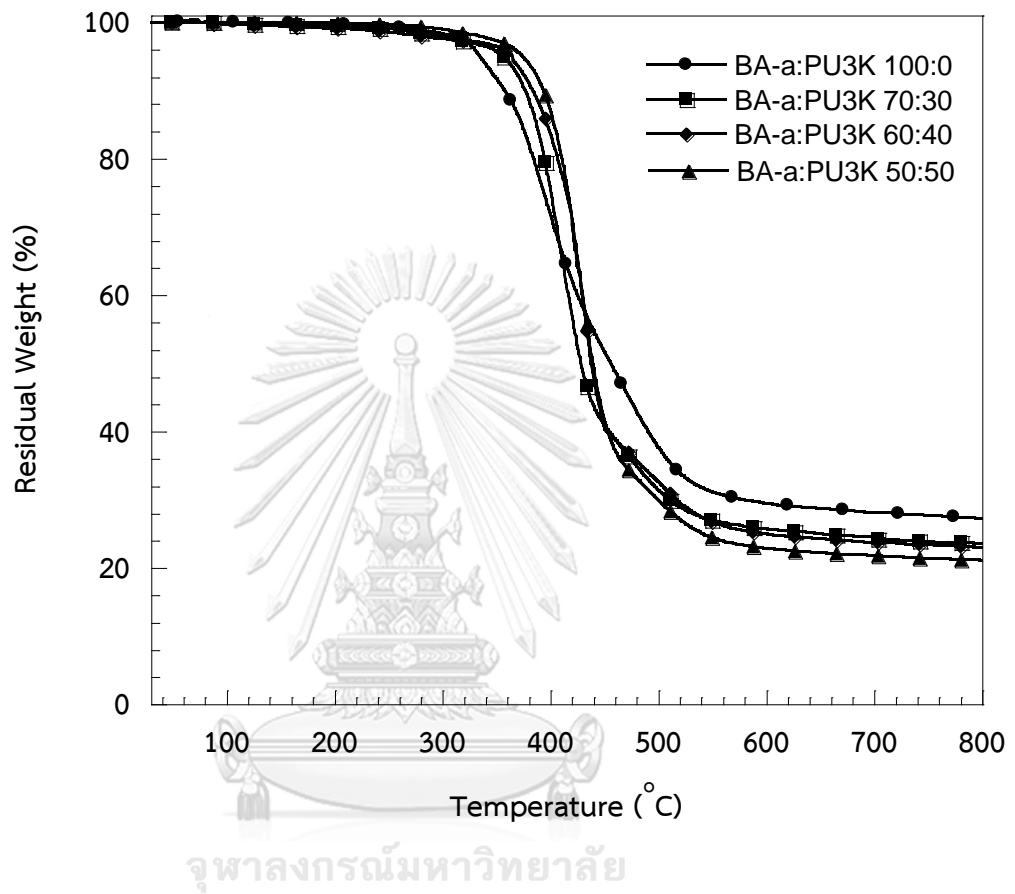


Figure 3.8 TGA thermograms of BA-a/PU3K alloys at various compositions:

(●)100:0, (■)70:30, (◆)60:40 and (▲)50:50

REFERENCES



จุฬาลงกรณ์มหาวิทยาลัย
CHULALONGKORN UNIVERSITY

- [1] Linegar, K.L. Applications of dynamic light scattering in chemical and biomolecular engineering: Polymers, Proteins and Liquid Crystals. Master of Science, Institute for Physical Science and Technology and Department of Chemical and Biomolecular Engineering, University of Maryland,, 2008.
- [2] Nitz, P. and Hartwig, H., Solar control with thermotropic layers. Solar Energy, 2005. 79(6): p. 573-582.
- [3] Mucha, M., Polymer as an important component of blends and composites with liquid crystals. Progress in Polymer Science, 2003. 28(5): p. 837-873.
- [4] Hoppe, C., Galante, M., Oyanguren, P., and Williams, R., Thermally reversible light scattering films based on droplets of a liquid crystal (N-4-ethoxybenzylidene-4'-n-butylaniline)/polystyrene solution dispersed in an epoxy matrix. Macromolecules, 2004. 37(14): p. 5352-5357.
- [5] McIntyre, W.D. and Soane, D.S., Controlled phase separation of polymer-liquid crystal mixtures for reversible optical data storage. Applied optics, 1990. 29(11): p. 1658-1665.
- [6] Buckley, G. and Roland, C., Reversible optical data storage on poly (ethylene terephthalate). Polymer Engineering & Science, 1997. 37(1): p. 138-142.
- [7] Wang, J., Xia, J., Hong, S.W., Qiu, F., Yang, Y., and Lin, Z., Phase separation of polymer-dispersed liquid crystals on a chemically patterned substrate. Langmuir, 2007. 23(14): p. 7411-7415.
- [8] Zucchi, I.A., Galante, M.J., and Williams, R.J., Thermally reversible light scattering films based on the melting/crystallization of organic crystals dispersed in an epoxy matrix. European polymer journal, 2006. 42(4): p. 815-822.
- [9] Tercjak, A., Serrano, E., and Mondragon, I., Thermally reversible materials based on thermosetting systems modified with polymer dispersed liquid crystals for optoelectronic application. Polymers for advanced technologies, 2006. 17(11-12): p. 835-840.
- [10] Tercjak, A. and Mondragon, I.a., Relationships between the morphology and thermoresponsive behavior in micro/nanostructured thermosetting matrixes

- containing a 4'-(hexyloxy)-4-biphenylcarbonitrile liquid crystal. Langmuir, 2008. 24(19): p. 11216-11224.
- [11] Raicu, A., Wilson, H.R., Nitz, P., Platzer, W., Wittwer, V., and Jahns, E., Facade systems with variable solar control using thermotropic polymer blends. Solar Energy, 2002. 72(1): p. 31-42.
- [12] Seeboth, A., Löttsch, D., and Potechius, E., Phase transitions and phase separations in aqueous polyether systems. Colloid & Polymer Science, 2001. 279(7): p. 696-704.
- [13] Chung, W.Y., Lee, S.M., Koo, S.M., and Suh, D.H., Surfactant-free thermochromic hydrogel system: PVA/borax gel networks containing pH-sensitive dyes. Journal of applied polymer science, 2004. 91(2): p. 890-893.
- [14] Zalba, B., Marín, J.M., Cabeza, L.F., and Mehling, H., Review on thermal energy storage with phase change: materials, heat transfer analysis and applications. Applied thermal engineering, 2003. 23(3): p. 251-283.
- [15] Takahashi, Y., Tamaoki, N., Komiya, Y., Hieda, Y., Koseki, K., and Yamaoka, T., Thermo-optic effects of 4-alkoxy-3-chlorobenzoic acids in polymeric matrices. Journal of applied physics, 1993. 74(6): p. 4158-4162.
- [16] Tercjak, A., Serrano, E., Garcia, I., Ocando, C., and Mondragon, I., Self-assembled block copolymers as matrix for multifunctional materials modified with low-molecular-weight liquid crystals. Acta Materialia, 2007. 55(19): p. 6436-6443.
- [17] Rimdusit, S., Jubsilp, C., and Tiptipakorn, S., Alloys and Composites of Polybenzoxazines. 2013, Singapore: Springer.
- [18] Takeichi, T. and Guo, Y., Preparation and properties of poly (urethane-benzoxazine) s based on monofunctional benzoxazine monomer. Polymer journal, 2001. 33(5): p. 437-443.
- [19] Takeichi, T., Guo, Y., and Agag, T., Synthesis and characterization of poly (urethane-benzoxazine) films as novel type of polyurethane/phenolic resin composites. Journal of Polymer Science Part A: Polymer Chemistry, 2000. 38(22): p. 4165-4176.

- [20] Rimdusit, S., Pirstpindvong, S., Tanthapanichakoon, W., and Damrongsakkul, S., Toughening of polybenzoxazine by alloying with urethane prepolymer and flexible epoxy: A comparative study. Polymer Engineering & Science, 2005. 45(3): p. 288-296.
- [21] Thassu, D. and Chader, G.J., Ocular Drug Delivery Systems: Barriers and Application of Nanoparticulate Systems Deepak Thassu, Gerald J. Chader. 2012, United States of America: Taylor & Francis Group.
- [22] Seeboth, A. and Löttsch, D., Thermochromic and Thermotropic Materials. 2013, United States of America: Pan Stanford.
- [23] Nair, C.P.R., Advances in addition-cure phenolic resins. Progress in Polymer Science, 2004. 29(5): p. 401-498.
- [24] Ning, X. and Ishida, H., Phenolic materials via ring-opening polymerization: Synthesis and characterization of bisphenol-A based benzoxazines and their polymers. Journal of Polymer Science Part A: Polymer Chemistry, 1994. 32(6): p. 1121-1129.
- [25] Reiss, G., Schwob, J., Guth, G., Roche, M., and Lande, B., Advances in polymers Synthesis. 1985, New York: Plenum press.
- [26] Takeichi, T., Guo, Y., and Rimdusit, S., Performance improvement of polybenzoxazine by alloying with polyimide: effect of preparation method on the properties. Polymer, 2005. 46(13): p. 4909-4916.
- [27] Wood, G., The ICI polyurethanes book, ed. 1. 1987, Singapore: John Wiley&Sons.
- [28] Randall, D. and Lee, S., The Polyurethanes Handbook. 2002, United Kingdom: John Wiley&Sons.
- [29] Ionescu, M., *Chemistry and Technology of Polyols for Polyurethanes*, 2005, Smithers Rapra Technology.
- [30] Hepburn, C., Polyurethane Elastomers. 1992: Springer Netherlands.
- [31] Wood, G., The ICI polyurethanes book, ed. 2. 1990, Singapore: John Wiley&Sons.

- [32] Wiseman, P., Raw materials for industrial polymers H. Ulrich, Hanser Publishers, Munich, 1988. pp. 223, price DM84. 00. ISBN 3-446-15099-4. Polymer International, 1989. 21(4): p. 361-361.
- [33] Cao, L.-c., Mou, M., Feng, G., and Wang, Y.-c., Thermo-optical study of UV cured polyether urethane diacrylate films with dispersed octadecanol. European Polymer Journal, 2009. 45(9): p. 2587-2593.
- [34] Zucchi, I.A., Resnik, T., Oyanguren, P.A., Galante, M.J., and Williams, R.J.J., Comparison of optical properties of thermally reversible light scattering films consisting in dispersions of polystyrene/naphthalene domains or polystyrene/liquid crystal (EBBA) domains in epoxy matrices. Polymer Bulletin, 2006. 58(1): p. 145-151.
- [35] Kasemsiri, P., Wakita, J., Ando, S., and Rimdusit, S., *Thermally Reversible Light Scattering Characteristics of Benzoxazine-Urethane Alloy*, 2009, Tokyo Institute of Technology: Japan.
- [36] Puig, J., Williams, R.J.J., and Hoppe, C.E., Poly(dodecyl methacrylate) as Solvent of Paraffins for Phase Change Materials and Thermally Reversible Light Scattering Films. ACS Applied Materials & Interfaces, 2013. 5(18): p. 9180-9185.
- [37] Rimdusit, S., Mongkhonsi, T., Kamonchaivanich, P., Sujirote, K., and Thiptipakorn, S., Effects of polyol molecular weight on properties of benzoxazine-urethane polymer alloys. Polymer Engineering & Science, 2008. 48(11): p. 2238-2246.
- [38] Ishida, H. and Allen, D.J., Mechanical characterization of copolymers based on benzoxazine and epoxy. Polymer, 1996. 37(20): p. 4487-4495.
- [39] Andronescu, C., Bîru, E.I., Radu, I.C., Gârea, S.A., and Iovu, H., Kinetics of benzoxazine polymerization studied by Raman spectroscopy. High Performance Polymers, 2013. 25(6): p. 634-640.
- [40] Socrates, G., Infrared and Raman characteristic group frequencies: tables and charts. 2004: John Wiley & Sons.

- [41] Dunkers, J. and Ishida, H., Reaction of benzoxazine-based phenolic resins with strong and weak carboxylic acids and phenols as catalysts. Journal of Polymer Science Part A Polymer Chemistry, 1999. 37(13): p. 1913-1921.
- [42] Nielsen, L.E., Mechanical properties of polymers and composites, ed. 1st. 1974, New York: Marcel Dekker.
- [43] Cowie, J.M.G., Chemistry & Physics of Modern Materials. Polymer, ed. 2nd. 1991, New York: Chapman & Hall.



VITA

Mr. Kittipon Bunyanuwat was born in Bangkok, Thailand on January 5, 1990. He completed high school in 2008 from Wat Rajabohit School and graduated Bachelor degree from the Department of Chemical Engineering, Faculty of Engineering, King Mongkut's University of Technology Thonburi, Thailand in 2012. After graduation, he continued his work for an Indorama Ventures Public Company Limited. After that, he resigned his work and continued his study for a Master's Degree of Chemical Engineering at the Department of Chemical Engineering, Faculty of Engineering, Chulalongkorn University

Some part of this work was selected for oral presentation at The 6th International Thai Institute of Chemical Engineering and Applied Science Conference or ITIChE 2016 on October 26-28, 2016 at Thailand Science Park Convention Center, Bangkok, Thailand and the The 7th International Thai Institute of Chemical Engineering and Applied Science Conference or ITIChE 2017 on October 18-20, 2017 at the Shangri-La Hotel, Bangkok, Thailand.



จุฬาลงกรณ์มหาวิทยาลัย
CHULALONGKORN UNIVERSITY